DESY 08–182
December 2008

arXiv:0812.1245v1 [physics.data-an] 5 Dec 2008

Mathematical Framework for Fast and Rigorous Track Fit for the ZEUS Detector

Alexander Spiridonov[*]
DESY

Abstract

In this note we present a mathematical framework for a rigorous approach to a common track fit for trackers located in the inner region of the ZEUS detector. The approach makes use of the Kalman filter and offers a rigorous treatment of magnetic field inhomogeneity, multiple scattering and energy loss. We describe mathematical details of the implementation of the Kalman filter technique with a reduced amount of computations for a cylindrical drift chamber, barrel and forward silicon strip detectors and a forward straw drift chamber. Options with homogeneous and inhomogeneous field are discussed. The fitting of tracks in one ZEUS event takes about of 20 ms on standard PC.

[*]E-mail: Alexander.Spiridonov@desy.de
Permanent address: Institute of Theoretical and Experimental Physics, 117259 Moscow, Russia

Contents

1 Introduction **4**

2 Overview of the tracker layout **4**

3 Track Models and Likelihood Functions in a Multi-Component Tracker **5**

4 Application of the Kalman filter technique to track fitting **8**
4.1 Linear Model 9
4.2 Non–linear Model 10

5 Particle Motion in a Static Magnetic Field **10**

6 Multiple Scattering and Energy Loss **11**

7 Specifics of Kalman Filter Implementation for the ZEUS Inner Trackers **12**

8 Cylindrical Parameterization for central tracks **13**
8.1 Cylindrical Parameterization: Prediction Equations 15
8.2 Cylindrical Parameterization: Projection of State Vector to MVD Measurement 16
8.3 Cylindrical Parameterization: Projection of State Vector to CTD Measurement 17
8.4 Cylindrical Parameterization: Process Noise 19

9 Cartesian Parameterization in an Inhomogeneous Magnetic Field **20**
9.1 Cartesian Parametrization: Equations of Motion in Inhomogeneous Magnetic Field 20
9.2 Cartesian Parametrization: Equations for Derivatives 21
9.3 Cartesian Parameterization: Projection of State Vector to MVD Measurement 22
9.4 Cartesian Parameterization: Projection of State Vector to CTD Measurement 23
9.5 Cartesian Parameterization: Projection of State Vector to STT Measurement 25
9.6 Cartesian Parameterization: Process Noise 26
9.7 Cartesian Parameterization for Rear Tracks 26

10 Global Parameterization **27**

11 Fast Computations with Kalman Filter Technique **27**

12 Conclusions **30**

References **30**

13 Appendix A: Jacobian of prediction transformation in cylindrical parameterization **32**

14 Appendix B: Jacobian of projection transformation for the CTD in cylindrical parameterization **33**

15 Appendix C: Jacobian of projection transformation for the CTD in cartesian parameterization **34**

16 Appendix D: Conversions from Local to Global Parameters **34**

1 Introduction

The ZEUS experiment [1] was operated at the electron-proton collider HERA at DESY until 2007. The ZEUS detector was a sophisticated, multi-component tool for studying particle reactions provided by electron-proton collisions with an energy 27.5 GeV and 920 GeV,respectively. The inner tracking components of the ZEUS detector were: the silicon strip Micro Vertex Detector [2] with barrel (BMVD) and forward (FMVD) parts; the Central Tracking Detector (CTD) [3] consisting of the cylindrical drift chamber; the Forward Tracking Device (FTD) [1] and the forward Straw-Tube Tracker (STT) [4]. The MVD was located in the vicinity of interaction point, inside of the CTD.

The magnetic field in the central region of the ZEUS detector was produced by a thin superconducting solenoid. The field had a strength of 14.3 kGauss at the center and was directed parallel to the proton beam. The barrel MVD and CTD were located in the field which was almost homogeneous with a small radial component far from the center. Forward trackers were placed outside of the solenoid or close to its edge where the field is inhomogeneous.

We consider a mathematical framework for a rigorous approach to a common track fit, which can be performed with tracks including all inner tracking components or with any combination of them. The approach offers a rigorous treatment of field inhomogeneity, multiple scattering and energy loss. The track fitting procedure makes use of the Kalman filter technique and we discuss how to optimize computations and make the fitting procedure fast.

2 Overview of the tracker layout

The ZEUS coordinate system is a right-handed Cartesian system, with the z–axis pointing in the proton beam direction (forward) and the x–axis pointing to the center of the HERA ring. The coordinate origin is at the nominal interaction point.

The barrel (BMVD) and forward (FMVD) section of the MVD includes 600 and 112 sensors, respectively [2]. A sensor is a silicon single-sided strip detector with a readout pitch of 120 μm which includes five innermost strips for capacitive charge division. The ZEUS MVD has 307,200 and 53,730 readout channels in the barrel and forward sections, respectively.

The barrel section, centered at the interaction point, is about 63 cm long. The silicon sensors are arranged in three concentric cylindrical layers with radii about 5 cm, 8 cm and 12 cm. Two back to back sensors in a layer provide measurements of nominal $r-\phi$ and z position. The FMVD is composed of four transverse disks of 14 wedges each, which extend the angular coverage down to 7° from the beam line. Each wedge has two sensor layers separated by approximately 8 mm in z–direction. They are mounted back to back, such that the angle between strips is $2 \times 13°$.

The CTD [2] is a cylindrical drift chamber, with a sensitive volume approximately 2m in length and 0.4 (1.6m) in inner (outer) diameter. The CTD wires are arranged into nine

concentric superlayers numbered consecutively from the inside out. The odd-numbered superlayers have sense wires running parallel to the chamber axis (i.e. z–axis) while those in the even-numbered superlayers have a 5° stereo angle. We denote sense wires in corresponding superlayers as axial and stereo, respectively. Each superlayer contains eight sense wire layers – there are 4608 sense wires in total. A set of eight sense wires is surrounded by field wires, azimuthally dividing a superlayer into cells of polygonal shape. Each sense wire is read out by a flash ADC and, finally a drift distance is evaluated for a hit. All axial wires in superlayer one and the odd numbered wires in superlayer three and five (in total 704 wires) are additionally equipped with the z-by-timing system, which measures z position of a hit.

The STT uses straw drift chambers with 7.5 mm diameter capton tubes of varying length from 20 cm to 75 cm. There are in total 10,944 wires in 48 wedge shaped sectors. Each wedge covers an azimuthal span of 60°. Each sector consists of 3 layers of straws perpendicular to the z–axis. A track crossing the STT nominally delivers 24 drift time measurements.

3 Track Models and Likelihood Functions in a Multi-Component Tracker

The likelihood function of a track measurement has a meaning regardless of the details of any fitting method. The maximum-likelihood estimator is *efficient* in the sense that no other unbiased estimator has smaller variances. A track model which is appropriate for the likelihood function, together with a given method of track fit, may produce an efficient estimate of parameters. A general point of view of the information delivered by a tracker can help to interpret behavior of variances of fitted parameters and hit residuals.

We can model a multi-component tracker by a set of track detecting elements and intermediate blocks of passive material, which are located in a static magnetic field. Track parameters in the detector element k are described by a vector x_k. For the case of a three-dimensional fit, the dimension of the vector,x_k, is 5. The track measurement in the tracker element k, i.e. the k^{th} hit, is a vector denoted by m_k. In general m_k is the vector with its dimension corresponding to that of the tracking element. For example, m_k has only 1 coordinate for a silicon strip of the MVD, a drift tube of the STT or a stereo wire of the CTD and 2 coordinates (drift time and z position of a hit) for an axial wire of the CTD which is additionally equipped with the z-by-timing system. The measurement error can be described by the covariance matrix V_k. We approximate the probability (density) of the measurement m_k given the vector of track parameters x_k

$$P(m_k|x_k) = G(m_k|\langle m_k\rangle; V_k) \tag{1}$$

by a Gaussian function with the mean value $\langle m_k\rangle$ and covariance matrix V_k:

$$G(m_k|\langle m_k\rangle; V_k) = C(V_k)\exp\Big\{-\frac{1}{2}(m_k-\langle m_k\rangle)^T V_k^{-1}(m_k-\langle m_k\rangle)\Big\}, \tag{2}$$

where $C(V_k)$ is a normalization constant. An operator H_k projects the actual vector x_k into the space of measurement:

$$\langle m_k \rangle = H_k \, x_k. \tag{3}$$

Suppose that we are interested in the track parameters at the beginning of track, x_1. The likelihood function takes the form of a product:

$$L(m_1, m_2, ..., m_N | x_1) = P(x_2, ..., x_N | x_1) \cdot \prod_{k=1}^{N} G(m_k | H_k \, x_k; V_k). \tag{4}$$

The first term is the probability for a particle to pass through the points $x_2, ..., x_N$ given the parameters x_1 at the beginning and the second one is the probability to obtain the measurements, $m_1, ..., m_N$, while measuring the points in the space of track parameters $x_1, ..., x_N$ of the real (not the mean) trajectory. The probability, $P(x_2, ..., x_N | x_1)$, can be approximated by a Gaussian distribution

$$P(x_2, ..., x_N | x_1) = G(x_2, ..., x_N | \langle x_2(x_1) \rangle, ..., \langle x_N(x_1) \rangle; \Sigma(x_1)). \tag{5}$$

The mean trajectory is defined as:

$$\langle x_k(x_1) \rangle = \mathcal{F}_k x_1, \tag{6}$$

where the operator $\mathcal{F}_k$ swims track parameters x_1 into the detector element k. The track model may be described as a continuous curve for the mean trajectory with fluctuations of actual parameters x_k with respect to the mean trajectory,

$$\mathcal{D}_k(x_1) = x_k - \mathcal{F}_k x_1. \tag{7}$$

The fluctuation, $\mathcal{D}_k(x_1)$, accumulates the effect of multiple scattering on the pass from the beginning of the track to the given element. Vectors $\{\mathcal{D}_k(x_1)\}$ are correlated and, therefore, matrix $\Sigma(x_1)$ has dense structure (many non-zero elements). We can combine Gaussian functions from (4) and (5):

$$L(m_1, m_2, ..., m_N | x_1) = G(m_1, m_2, ..., m_N | H_1 x_1, H_2 \mathcal{F}_2 x_1, ..., H_N \mathcal{F}_N x_1; \mathcal{M}(x_1)), \tag{8}$$

where the non-diagonal covariance matrix $\mathcal{M}(x_1)$ has dimension equal to the sum of dimensions of all measurements $\{m_k\}$. The dimension of the $\mathcal{M}$ may be of order 10^2 for modern tracking detectors. Maximization of the likelihood function of Gaussian type, i.e. least square fitting with large non-diagonal covariance matrix $\mathcal{M}$, requires a lot of computations, although not more than 5 parameters are fitted. Because of large computing time, the model is not convenient for a track fitting in a multi-component tracker. But the model includes a small number of fitted parameters, and is suitable for a subsequent update of detector alignment parameters [5], where an expansion of hit residuals w.r.t. fitted parameters is needed.

A charged particle traversing a medium can be described by a stochastic process with the Markov property and, therefore, the conditional probability distribution of future

states depends only upon the present state and not on any past states. The probability function for a particle to pass through the points $x2, ..., x_N$ in (5) can be rewritten as:

$$P(x_2, ..., x_N|x_1) = \prod_{k=2}^{N} P(x_k|x_{k-1}) = \prod_{k=2}^{N} G(x_k|\langle x_k(x_{k-1})\rangle; Q_k(x_{k-1})). \tag{9}$$

We approximate the conditional probability (density), $P(x_k|x_{k-1})$, for track parameters x_k, given the parameters in the previous state x_{k-1}, by the Gaussian distribution, $G(x_k|\langle x_k(x_{k-1})\rangle; Q_k(x_{k-1}))$ with the mean $\langle x_k(x_{k-1})\rangle$ and covariance matrix $Q_k(x_{k-1})$. The mean trajectory in the tracking element k is

$$\langle x_k(x_{k-1})\rangle = F_k x_{k-1}. \tag{10}$$

The operator F_k swims track parameters x_{k-1} into the detector element k according to the equations of motion.

Suppose that we are interested in track parameters in all points of track measurement, i.e. $x_1, x_2, ..., x_N$. The likelihood function takes a form:

$$L(m_1, ..., m_N|x_1, ..., x_N) = G(m_1|H_1\, x_1; V_1) \cdot \prod_{k=2}^{N} G(x_k|F_k\, x_{k-1}; Q_k)\, G(m_k|H_k\, x_k; V_k), \tag{11}$$

with Gaussian functions

$$G(m_k|H_k\, x_k; V_k) = C(V_k) \exp\Big\{ -\frac{1}{2}(m_k - H_k\, x_k)^T V_k^{-1} (m_k - H_k\, x_k)\Big\} \tag{12}$$

and

$$G(x_k|F_k\, x_{k-1}; Q_k) = C(Q_k) \exp\Big\{ -\frac{1}{2}(x_k - F_k\, x_{k-1})^T Q_k^{-1} (x_k - F_k\, x_{k-1})\Big\}, \tag{13}$$

where $C(V_k)$ and $C(Q_k)$ are normalization constants.

The model for the total track is not a continuous curve, but consists of $N-1$ continuous segments. A variation of track parameters in the point of discontinuity

$$\delta_k = x_k - F_k x_{k-1} \tag{14}$$

describes the effect of multiple scattering on the pass from the the previous element $k-1$ to the element k. Vectors $\{\delta_k\}$ are uncorrelated. A spread of the δ_k is defined by the covariance matrix Q_k.

The maximum likelihood estimation of parameters $\{x_k\}$ satisfies the system of equations

$$\left\{ \frac{\partial\,(-\ln L)}{\partial x_k^T} \;=\; 0 \right\}. \tag{15}$$

If operators F_k and H_k are non-linear (e.g. in magnetic field) then the latter equations are non-linear also. The problem can be solved iteratively using the well known method of linearization of operations (3) and (10). Anyhow we can regard the functional,

$\partial(-\ln L)/\partial x_k^T$, as a linear form w.r.t. vectors of estimated parameters $\{x_k\}$. The vector, x_k, associates in (11) only with vectors in neighboring data points $k-1$ and $k+1$ and, therefore, the linear form $\partial(-\ln L)/\partial x_k^T$ includes only 3 terms with vectors x_{k-1}, x_k and x_{k+1}[1], respectively. Finally, the system (15) looks as

$$\begin{pmatrix} I_{11} & I_{12} & & & & & \\ I_{21} & I_{22} & I_{23} & & & & \\ & I_{32} & I_{33} & I_{34} & & & \\ & & \dots & \dots & \dots & & \\ & & & \dots & \dots & \dots & \\ & & & & I_{N-1\,N} & I_{NN} \end{pmatrix} \begin{pmatrix} x_1 \\ x_2 \\ x_3 \\ \dots \\ \dots \\ x_N \end{pmatrix} = \begin{pmatrix} r_1 \\ r_2 \\ r_3 \\ \dots \\ \dots \\ r_N \end{pmatrix}, \tag{16}$$

where submatrices related to points i, j,

$$I_{ij} = \frac{\partial^2(-\ln L)}{\partial x_i^T \partial x_j},$$

are parts of the information matrix. The sparse (with many zero elements), band structure of the information matrix can be exploited to reduce computations drastically. This can be achieved by using either a dedicated algorithm of matrix inversion [6], or else (e.g. in the broken lines fit [7]) by the matrix (Cholesky) decomposition into a unit triangle, U, and a diagonal, D, matrix

$$U\,D\,U^T\mathbf{x} = \mathbf{r}$$

which requires two steps to solve for $\mathbf{x}$:

$$U\,\mathbf{y} = \mathbf{r} \quad \text{and} \quad D\,U^T\mathbf{x} = \mathbf{y}.$$

The track model based on relations (10 – 14) is well suited also for an implementation of the progressive track fit by the method [8] or for the application of the Kalman filter formalism [9]. Both methods are rather economical regarding computing time because they include operations with matrices of maximal size 5 by 5 for each hit.

4 Application of the Kalman filter technique to track fitting

In [9] it was shown that an appropriate mathematical framework for the iterative procedure of track fitting is the theory of linear filtering, in particular the Kalman filter [10]. To consider the mathematical framework of a Kalman filter, we try to follow the notation used in [11]. In the following we describe a case with a linear system and a non-linear system will be discussed at Subsec. 4.2.

[1] Differentiating the latter linear form with respect to x_i isolates a coefficient in a corresponding linear term.

4.1 Linear Model

The Kalman filter proceeds progressively from one measurement to the next and improves the knowledge about the particle trajectory by updating the track parameters with each new measurement. The system state vector (track parameters) after inclusion of $k-1$ measurements is denoted by $\tilde{x}_{k-1}$, and its covariance matrix by C_{k-1}. The state vector and its covariance matrix are propagated to the location of the next measurement with the *prediction equations*:

$$\tilde{x}_k^{k-1} = F_k \tilde{x}_{k-1}, \tag{17}$$

and

$$C_k^{k-1} = F_k C_{k-1} F_k^T + Q_k, \tag{18}$$

where F_k is the transport matrix and Q_k denotes the covariance matrix of the *process noise*, which occurs due to the random perturbation of the particle's trajectory.

The measurement of the vector $\tilde{x}_k^{k-1}$ and its covariance matrix are denoted by m_k and V_k, respectively. The *expected* measurement m_k is described by the projection matrix H_k. The estimated residuals are

$$r_k^{k-1} = m_k - H_k\, \tilde{x}_k^{k-1} \tag{19}$$

and its covariance matrix become:

$$R_k^{k-1} = V_k + H_k\, C_k^{k-1}\, H_k^T. \tag{20}$$

The updating of the system state vector after inclusion of the measurement k is defined by the *filter equations*:

$$\begin{aligned} K_k &= C_k^{k-1}\, H_k^T\, (R_k^{k-1})^{-1}, \\ \tilde{x}_k &= \tilde{x}_k^{k-1} + K_k\, r_k^{k-1}, \\ C_k &= (1 - K_k\, H_k)\, C_k^{k-1}, \end{aligned} \tag{21}$$

with the filtered residuals and its covariance matrix

$$r_k = (1 - H_k\, K_k)\, r_k^{k-1}, \qquad R_k = (1 - H_k\, K_k)\, V_k = V_k - H_k C_k H_k^T. \tag{22}$$

The matrix, K_k, is called the *filtering (gain) matrix*. The filtered state vector is pulled towards the measurement and, therefore the quadratic mean of the filtered residual is smaller than the measurement error. The χ^2 increment after the filtering of the state vector is given by:

$$\chi_k^2 = r_k^T\, R_k^{-1}\, r_k.$$

The track parameters after the filtering procedure are known with optimal precision only at the last point of the fit. The smoothing part of the Kalman filter is a very useful complement, which solves the problem of optimal parameter estimation at every point of the trajectory. The smoothing is also a recursive procedure which proceeds step by step

in the direction opposite to that of the filter with the *smoother equations*:

$$\begin{aligned}
A_k &= C_k\, F_{k+1}^T\, (C_{k+1}^k)^{-1}, \\
\tilde{x}_k^n &= \tilde{x}_k + A_k(\tilde{x}_{k+1}^n - \tilde{x}_{k+1}^k), \\
C_k^n &= C_k + A_k(C_{k+1}^n - C_{k+1}^k)A_k^T, \\
r_k^n &= m_k - H_k\tilde{x}_k^n, \\
R_k^n &= R_k - H_k A_k(C_{k+1}^n - C_{k+1}^k)A_k^T H_k^T = V_k - H_k C_k^n H_k^T.
\end{aligned} \tag{23}$$

The smoothed state vector, $\tilde{x}_k^n$, is more precise, because it includes information from all measurements. The variance of the smoothed state vector, C_k^n, is smaller than the variance of the filtered state vector, C_k. The quadratic mean of the smoothed residual is closer to the measurement error (detector resolution) than the filtered one.

4.2 Non–linear Model

A particle's motion in a detector with magnetic field is a nonlinear process. In case of a non-linear system, we have to replace the transport, F_k, and projection, H_k, matrices in (17) and (19), respectively, by exact non-linear functions:

$$\tilde{x}_k^{k-1} = f_k(\tilde{x}_{k-1}), \qquad\qquad r_k^{k-1} = m_k - h_k(\tilde{x}_k^{k-1}). \tag{24}$$

Jacobian matrices of these functions (Jacobians in the following)

$$\frac{\partial(f_k)}{\partial(\tilde{x}_{k-1})}, \qquad\qquad \frac{\partial(h_k)}{\partial(\tilde{x}_k^{k-1})} \tag{25}$$

will be used in equations for covariance matrix propagation (18) and (20) instead of F_k and H_k, respectively. In practice, estimation with Kalman filter for a non-linear system shows properties similar to those of maximum-likelihood estimation:

- The estimator is asymptotically unbiased, i.e. its bias tends to zero as the number of measurements increases.
- The distribution of deviations of estimated parameters from true values approaches a Gaussian distribution also asymptotically, i.e for sufficiently large number of measurements.

5 Particle Motion in a Static Magnetic Field

The equation of motion of a particle with momentum $\vec{p}$ (velocity $\vec{v}$) and charge Q in a static magnetic field $\vec{B}$ is:

$$\frac{d\,\vec{p}}{d\,t} = \kappa \cdot Q \cdot \vec{v} \times \vec{B}, \tag{26}$$

where coordinates x, y, z are in cm, p is in GeV/c, the magnetic field B is in kGauss, and parameter κ is equal:

$$\kappa = 0.000299792458 \ (\mathrm{GeV/c})\,\mathrm{kG}^{-1}\,\mathrm{cm}^{-1}.$$

The distance along the trajectory of a particle (path length) is given by:

$$s = |\vec{v}| \cdot t.$$

The unitary vector $\vec{n}$ pointing along the direction of the trajectory is:

$$\vec{n} = \frac{d\,\vec{x}}{d\,s}. \tag{27}$$

Equation (26) can be rewritten as:

$$\frac{d\,\vec{n}}{d\,s} = \kappa \cdot \frac{Q}{|\vec{p}|} \cdot \vec{n} \times \vec{B} = \kappa \cdot q \cdot \vec{n} \times \vec{B}, \tag{28}$$

where $q = Q/|\vec{p}|$. The latter equation combined with Eq. (27) gives a system of linear differential equations:

$$\begin{aligned}
d\,x\,/\,d\,s &= n_x, \\
d\,y\,/\,d\,s &= n_y, \\
d\,z\,/\,d\,s &= n_z, \\
d\,n_x\,/\,d\,s &= \omega_z \cdot n_y - \omega_y \cdot n_z, \\
d\,n_y\,/\,d\,s &= \omega_x \cdot n_z - \omega_z \cdot n_x, \\
d\,n_z\,/\,d\,s &= \omega_y \cdot n_x - \omega_x \cdot n_y, \\
q &= \mathrm{const},
\end{aligned} \tag{29}$$

where $\omega_i(s) = \kappa \cdot q \cdot B_i(\vec{x}(s))$.

6 Multiple Scattering and Energy Loss

The ZEUS inner tracking detectors were designed using minimal material. We take account of the effect of multiple scattering in the approximation of thin scatterers. Multiple scattering after traversing a material of small thickness, l, results in the perturbation of angles and coordinates, but the effect on the latter has an additional order of smallness $o(l)$ and can be neglected. The deflection of the particle momentum $\vec{p}$ due to multiple scattering is decomposed into deflections in two orthogonal planes. We define two unit vectors $\vec{n_1}$, $\vec{n_2}$ which in combination with $\vec{n}$ form a right-handed Cartesian system:

$$\vec{n_1} = \frac{\vec{e_z} \times \vec{n}}{|\vec{e_z} \times \vec{n}|} = \frac{1}{n_t} \begin{pmatrix} -n_y \\ n_x \\ 0 \end{pmatrix}, \ \vec{n_2} = \vec{n_1} \times \vec{n} = \frac{1}{n_t} \begin{pmatrix} n_x \cdot n_z \\ n_y \cdot n_z \\ -n_t^2 \end{pmatrix}, \ \text{with}\, n_t = \sqrt{n_x^2 + n_y^2}. \tag{30}$$

The direction of the momentum after the scattering is:

$$\vec{n}\,' = \vec{n} + \theta_1 \cdot \vec{n_1} + \theta_2 \cdot \vec{n_2}, \tag{31}$$

where θ_1, θ_2 are random variables with

$$< \theta_{1,2} >= 0, \ \mathrm{var}\,(\theta_{1,2}) \ = \ \theta_{ms}^2, \ \mathrm{cov}(\theta_1, \theta_2) = 0. \tag{32}$$

Here θ_{ms} is the well-known Moliére theory expression for RMS of the deflection angle of a charged particle traversing a medium [15]

$$\theta_{ms}(t/X_0) = \frac{13.6\,\mathrm{MeV}}{\beta cp}\sqrt{t\,/X_0}\ \left[1 + 0.038\ln(t/X_0)\right], \tag{33}$$

where t/X_0 is the material thickness in radiation lengths, which has to account for the track inclination:

$$t = l \cdot \sqrt{1 + (n_x/n_z)^2 + (n_y/n_z)^2}. \tag{34}$$

We rewrite Eq. (31) for the deflection of components:

$$\delta\vec{n} \ = \ \begin{pmatrix} \delta n_x \\ \delta n_y \\ \delta n_z \end{pmatrix} = \theta_1 \begin{pmatrix} -n_y\,/\,n_t \\ n_x\,/\,n_t \\ 0 \end{pmatrix} \ + \ \theta_2 \begin{pmatrix} n_x \cdot n_z\,/\,n_t \\ n_y \cdot n_z\,/\,n_t \\ -n_t \end{pmatrix}. \tag{35}$$

Taking into account Eqs. (32), we derive:

$$\begin{array}{lcl} < \vec{n}\,' > & = & \vec{n}, \\ \mathrm{var}\,(n_x') & = & \theta_{ms}^2\,(n_y^2 + n_x^2 n_z^2)/n_t^2, \\ \mathrm{var}\,(n_y') & = & \theta_{ms}^2\,(n_x^2 + n_y^2 n_z^2)/n_t^2, \\ \mathrm{var}\,(n_z') & = & \theta_{ms}^2\,n_t^2, \\ \mathrm{cov}\,(n_x', n_y') & = & \theta_{ms}^2\,n_x\,n_y(n_z^2 - 1)/n_t^2, \\ \mathrm{cov}\,(n_x', n_z') & = & -\theta_{ms}^2\,n_x\,n_z, \\ \mathrm{cov}\,(n_y', n_z') & = & -\theta_{ms}^2\,n_y\,n_z. \end{array} \tag{36}$$

An ionization energy loss is regarded as a deterministic correction to a track energy. In the approximation of thin scatterer, track energy, E, after the traversal of a material is:

$$E' = E - (dE/dx)_{ion} \cdot t, \tag{37}$$

where $(dE/dx)_{ion}$ is the mean rate of ionization energy loss in the material.

7 Specifics of Kalman Filter Implementation for the ZEUS Inner Trackers

Seven equations (29) describe a particle motion in a magnetic field, although five parameters suffice to define the trajectory at any point. A suitable track parameterization may depend on the detector geometry and field shape. The magnetic field in the central part of the ZEUS detector is directed parallel to the z–axis. For the large part of the MVD the field is almost homogeneous with only a small radial component ($< 1\%$ at the edge of the

BMVD). For the most forward parts of the CTD and FMVD the inhomogeneity is larger, with reduction of the axial component by 8% and increasing of the radial component up to 15%. The STT detector is located outside the superconducting solenoid where the field is inhomogeneous. We choose a different way to proceed depending on the polar angle,θ, of a track ($\tan\theta = p_t/p_z$):

- we use an option with inhomogeneous field for "forward" tracks ($0 < \theta < 60^\circ$);
- a homogeneous field model is used for "central" tracks ($60^\circ < \theta < 120^\circ$);
- an inhomogeneous field is used also for "rear" tracks ($120^\circ < \theta < 180^\circ$).

The set of measurements, $\{m_k\}$, with its covariance matrices, $\{V_k\}$, and the map of magnetic field, $\vec{B}$, are input for the track fit. To develop a mathematical framework for Kalman filter implementation we have to make the following steps:

- Select a convenient parameterization of the state vector, x_k.
- Find a solution of the prediction equations, $f_k(x_{k-1})$, and a function to project the vector x_k to the measurement, $h_k(x_k)$.
- Obtain Jacobians of latter functions
$$\frac{\partial(f_k)}{\partial(x_{k-1})}, \quad \frac{\partial(h_k)}{\partial(x_k)}.$$
- Define covariance matrix of the process noise, Q_k.

8 Cylindrical Parameterization for central tracks

The magnetic field at the central region of the ZEUS superconducting solenoid is nearly parallel to the z–axis ($B_x, B_y \approx 0$) and has almost constant strength. Therefore we approximate it as homogeneous on the path from one point to the next. The system of equation (29) looks as

$$\begin{aligned} d\,x\,/\,d\,s &= n_x, \\ d\,y\,/\,d\,s &= n_y, \\ d\,z\,/\,d\,s &= n_z, \\ d\,n_x\,/\,d\,s &= \omega_z \cdot n_y \\ d\,n_y\,/\,d\,s &= -\omega_z \cdot n_x, \\ d\,n_z\,/\,d\,s &= 0 \\ q &= \text{const}, \end{aligned} \tag{38}$$

where $\omega_z = \kappa \cdot q \cdot B_z$. The component n_z is constant and the angle (azimuthal), ϕ, of the track direction with the x–axis depends linearly on s:

$$\begin{aligned} \phi(s) &= \phi_0 - \omega_z s, \\ n_x(s) &= n_t\,\cos(\phi_0 - \omega_z s), \\ n_y(s) &= n_t\,\sin(\phi_0 - \omega_z s), \\ n_z(s) &= n_{z0}, \end{aligned} \tag{39}$$

where ϕ_0, n_{z0} are initial values at $s = 0$. A pair of conserved quantities can be derived from (38):

$$\begin{aligned} x(s) + \frac{1}{\omega_z}\, n_y(s) &= x_0 + \frac{1}{\omega_z}\, n_{y0}, \\ y(s) - \frac{1}{\omega_z}\, n_x(s) &= y_0 - \frac{1}{\omega_z}\, n_{x0}, \end{aligned} \tag{40}$$

with initial values, x_0, y_0, n_{x0}, n_{y0}. Coordinates can by expressed via the track direction:

$$\begin{aligned} x(s) &= x_0 - \frac{1}{\omega_z}\, n_y(s) + \frac{1}{\omega_z}\, n_{y0}, \\ y(s) &= y_0 + \frac{1}{\omega_z}\, n_x(s) - \frac{1}{\omega_z}\, n_{x0}. \end{aligned} \tag{41}$$

In a homogeneous field, the particle trajectory is a helix. For the case of axial (cylindrical) symmetry, a natural replacement of particle coordinates, x and y, are the radius, r, and the $r\varphi$–coordinate at radius r, which we denote as u. The relation between these pairs of parameters reads:

$$\begin{aligned} x &= r \cos \frac{u}{r}, \\ y &= r \sin \frac{u}{r}, \end{aligned} \tag{42}$$

and

$$\begin{aligned} r &= \sqrt{x^2 + y^2}, \\ u &= r \arctan \frac{y}{x} = 2r \arctan \frac{y}{r + x} = 2r \arctan \frac{r - x}{y}. \end{aligned} \tag{43}$$

With the usage of an arc-length in the xy-plane, s_t, corresponding curvature ω and parameter $\lambda = \cot\theta$ (cotangent of the polar angle of the particle direction)

$$s_t = s \cdot n_t, \quad \omega = \frac{\omega_z}{n_t}, \quad \lambda = \frac{n_z}{n_t}, \tag{44}$$

we obtain the solution for particle coordinates:

$$\begin{aligned} x(t) &= r_0 \cos \frac{u_0}{r_0} - \frac{1}{\omega} \sin(\phi_0 - t) + \frac{1}{\omega} \sin \phi_0, \\ y(t) &= r_0 \sin \frac{u_0}{r_0} + \frac{1}{\omega} \cos(\phi_0 - t) - \frac{1}{\omega} \cos \phi_0, \\ z(t) &= z_0 + \frac{\lambda_0}{\omega} t, \\ t &= w \cdot s_t, \end{aligned} \tag{45}$$

where r_0, u_0 are values at $t = 0$. The particle which is located at a radius, r_0, given $t = 0$, then arrives at a radius, r, given the value of t, which satisfies the equation:

$$\begin{aligned} r^2 = \;& r_0^2 + T + S \sin\alpha - (S \sin\alpha + T) \cos t + S \cos\alpha \, \sin t, \\ & T = \frac{2}{\omega^2}, \quad S = \frac{2r_0}{\omega}, \quad \alpha = \phi_0 - \frac{u_0}{r_0}. \end{aligned} \tag{46}$$

Solutions of the latter equation are

$$\begin{aligned} & t_{1,2} = 2 \arctan \left[\frac{S \cos\alpha}{D - 2\,T - 2\,S \, \sin\alpha} \left(1 \pm \sqrt{1 - \frac{D \cdot (D - 2\,T - 2\,S \, \sin\alpha)}{S^2 \cos^2\alpha}} \right) \right] \\ & D = r^2 - r_0^2 = \Delta r (2 r_0 + \Delta r), \;\; \Delta r = r - r_0. \end{aligned} \tag{47}$$

The solution t_2 (with minus sign) corresponds to a shorter path length. We describe a particle in a homogeneous magnetic field by a state vector at a reference cylindrical surface of radius r_k:

$$x_k^T = (u_k,\ z_k,\ \phi_k,\ \lambda_k,\ q_k)\,, \tag{48}$$

where

u_k = $r\varphi$–coordinate at radius r_k,
z_k = z-coordinate,
ϕ_k = angle of xy-projection of track direction with the x–axis,
λ_k = $\cot\theta$ at radius r_k,
q_k = Q/p_k, inverse momentum signed according to particle charge, Q.

Such cylindrical parameterization looks natural for the barrel tracking detectors. An analogous state vector was used for the implementation of the Kalman filter formalism for the ALEPH Time Projection Chamber [12].

8.1 Cylindrical Parameterization: Prediction Equations

In the prediction stage of the Kalman filter, the state vector x_k is propagated at the next reference radius, $r_{k+1} = r_k + \Delta r_k$. We obtain this transformation from (42–45):

$$\begin{aligned} u_{k+1} &= 2r_{k+1}\arctan\frac{y_{k+1}}{r_{k+1}+x_{k+1}} = r_{k+1}\arctan\frac{y_{k+1}}{x_{k+1}},\\ z_{k+1} &= z_k + \tfrac{\lambda_k}{\omega_k}t_k,\\ \phi_{k+1} &= \phi_k - t_k,\\ \lambda_{k+1} &= \lambda_k,\\ q_{k+1} &= q_k, \end{aligned} \tag{49}$$

where

$$\begin{aligned} x_{k+1} &= r_k\cos\frac{u_k}{r_k} - \frac{1}{\omega_k}\sin(\phi_k - t_k) + \frac{1}{\omega_k}\sin\phi_k\\ y_{k+1} &= r_k\sin\frac{u_k}{r_k} + \frac{1}{\omega_k}\cos(\phi_k - t_k) - \frac{1}{\omega_k}\cos\phi_k,\\ \omega_k &= \kappa\cdot B_{zk}\cdot q_k\cdot\sqrt{1+\lambda_k^2}. \end{aligned} \tag{50}$$

and the variable, t_k, is evaluated from (47). We approximate the Jacobian of this transformation as:

$$\partial(x_{k+1})\,/\,\partial(x_k) = \begin{pmatrix} \partial u_{k+1}/\partial u_k & \mathbf{0} & \partial u_{k+1}/\partial\phi_k & \partial u_{k+1}/\partial\lambda_k & \partial u_{k+1}/\partial q_k\\ \partial z_{k+1}/\partial u_k & \mathbf{1} & \partial z_{k+1}/\partial\phi_k & \partial z_{k+1}/\partial\lambda_k & \partial z_{k+1}/\partial q_k\\ \partial\phi_{k+1}/\partial u_k & \mathbf{0} & \mathbf{1} & \partial\phi_{k+1}/\partial\lambda_k & \partial\phi_{k+1}/\partial q_k\\ \mathbf{0} & \mathbf{0} & \mathbf{0} & \mathbf{1} & \mathbf{0}\\ \mathbf{0} & \mathbf{0} & \mathbf{0} & \mathbf{0} & \mathbf{1} \end{pmatrix}. \tag{51}$$

Elements of the Jacobian which always are very close to zero or unity, we set explicitly to 0 or 1, respectively. We exploit the sparse structure of the Jacobian to reduce computations, as will be discussed in Sect. 11. Nontrivial elements of the Jacobian are presented in appendix A.

8.2 Cylindrical Parameterization: Projection of State Vector to MVD Measurement

The origin of the local coordinate system of a MVD sensor is given by the vector $\vec{r}_c$. The unit vector, $\vec{n}$, is perpendicular to the sensor plane. We define the axis of measurement by the unit vector, $\vec{m}$, which is located in the sensor plane and is perpendicular to strips. A state vector x_k is defined at a cylindrical reference surface of a radius, r_k. We can define the radius, r_k, in such a way that the reference point will be close to the sensor. In the immediate vicinity of the reference point, we linearize equations (49,50) with respect to the variable, t_k:

$$\begin{aligned} x(t_k) &= x_k + \frac{t_k}{\omega_k}\cos\phi_k, \\ y(t_k) &= y_k + \frac{t_k}{\omega_k}\sin\phi_k, \\ z(t_k) &= z_{k+1} + \frac{\lambda_k}{\omega_k}\,t_k. \end{aligned} \tag{52}$$

A condition of the trajectory intersection with the sensor plane reads:

$$[\,(\vec{r}(t_k) - \vec{r}_c)\cdot\vec{n}\,] = 0. \tag{53}$$

The variable advance, Δt_k, to travel from the radius, r_k, to the sensor plane is:

$$\begin{aligned} \Delta t_k &= -\frac{b_k}{a_k}, \\ a_k &= \frac{n_x}{\omega_k}\cos\phi_k + \frac{n_y}{\omega_k}\sin\phi_k + \frac{n_z}{\omega_k}\lambda_k, \\ b_k &= (x_k - x_c)\,n_x + (y_k - x_c)\,n_y + (z_k - z_c)\,n_z. \end{aligned} \tag{54}$$

To obtain the expected measurement, $h_k(x_k)$, we project the position vector in the local frame, $\vec{r}(\Delta t_k) - \vec{r}_c$, to the measurement axis, $\vec{m}$:

$$\begin{aligned} h_k(x_k) &= [\,(\vec{r}(\Delta t_k) - \vec{r}_c)\cdot\vec{m}\,] \\ &= \frac{\Delta t_k}{\omega_k}\,c_k + (x_k - x_c)\,m_x + (y_k - y_c)\,m_y + (z_k - z_c)\,m_z, \\ c_k &= m_x\cos\phi_k + m_y\sin\phi_k + m_z\,\lambda_k. \end{aligned} \tag{55}$$

Elements of the Jacobian, $\partial(h_k)/\partial(x_k)$, are:

$$\begin{aligned}
\partial h_k/\partial u_k &= \frac{c_k}{\omega_k}\,\partial\Delta t_k/\partial u_k - m_x\frac{y_k}{r_k} + m_y\frac{x_k}{r_k},\\
\partial h_k/\partial z_k &= \frac{c_k\,n_z}{\omega_k\,a_k} + m_z,\\
\partial h_k/\partial \phi_k &= \frac{c_k}{\omega_k}\,\partial\Delta t_k/\partial\phi_k + \frac{\Delta t_k}{\omega_k}(-m_x\sin\phi_k + m_y\cos\phi_k),\\
\partial h_k/\partial \lambda_k &= \frac{\Delta t_k}{\omega_k}\left(-\frac{n_z\,c_k}{a_k\,\omega_k} + m_z\right),\\
\partial h_k/\partial q_k &= 0,
\end{aligned} \tag{56}$$

with derivatives of Δt_k

$$\begin{aligned}
\partial\Delta t_k/\partial u_k &= \frac{1}{a_k}\left(n_x\frac{y_k}{r_k} - n_y\frac{x_k}{r_k}\right),\\
\partial\Delta t_k/\partial\phi_k &= \frac{\Delta t_k}{a_k\,\omega_k}\,(n_x\,\sin\phi_k - n_y\,\cos\phi_k).
\end{aligned} \tag{57}$$

To exploit the sparse structure of the Jacobian and reduce computations we approximate the Jacobian for specific cases:

$$\begin{aligned}
\partial(h_k)/\partial(x_k) &= \left(\begin{array}{ccccc} \frac{\partial h_k}{\partial u_k} & \mathbf{1} & \frac{\partial h_k}{\partial\phi_k} & \frac{\partial h_k}{\partial\lambda_k} & \mathbf{0}\end{array}\right), \quad \text{for} \quad m_z \approx 1,\\
\partial(h_k)/\partial(x_k) &= \left(\begin{array}{ccccc} \frac{\partial h_k}{\partial u_k} & \mathbf{0} & \frac{\partial h_k}{\partial\phi_k} & \mathbf{0} & \mathbf{0}\end{array}\right), \quad \text{for} \quad m_z \approx 0.
\end{aligned} \tag{58}$$

8.3 Cylindrical Parameterization: Projection of State Vector to CTD Measurement

Each sense stereo wire runs at a small angle, α, and its location in the xy-plane at coordinate z is:

$$\vec{w} = \vec{r}_w + (z - z_c)\,\vec{r'}_w, \tag{59}$$

where z_c is the z–coordinate of the nominal center of the CTD . A "planar drift" approximation is used to render measurements in space [13]. Drift distance is measured along the "planar drift measurement axis", $\vec{m}$:

$$\begin{aligned}
m_x &= -n_y/|\vec{n}|,\\
m_y &= +n_x/|\vec{n}|,
\end{aligned} \tag{60}$$

which is obtained by rotating the vector, $\vec{n}$, through $+90°$. The vector $\vec{n}$ depends linearly on the z coordinate:

$$\vec{n} = \vec{p}_w + (z - z_c)\,\vec{p'}_w. \tag{61}$$

A state vector x_k is defined at a cylindrical reference surface of a radius, r_k. We define the radius, r_k, in a way that the reference point is close to the point where the trajectory

hits the planar drift plane. Close to the reference point, we use linearized equations of motion (52). A condition of the trajectory intersection with the planar drift plane reads:

$$[\,(\vec{r}(t_k) - \vec{w}) \cdot \vec{n}\,] = 0. \tag{62}$$

The variable advance, Δt_k, to travel from the radius, r_k, to the planar drift plane is a solution (of smallest absolute value) of a quadratic equation, $(\Delta t_k)^2\, a_k + \Delta t_k\, b_k + c_k = 0$:

$$\Delta t_{k1,2} = \frac{1}{2a_k}\left(-b_k \pm \sqrt{b_k^2 - 4\, a_k\, c_k}\right), \tag{63}$$

with coefficients

$$\begin{array}{ll}
a_k = A_{kx}\, p'_{wx} + A_{ky}\, p'_{wy}, & \\
b_k = A_{kx}\, \mathcal{P}_{kx} + B_{kx}\, p'_{wx} + A_{ky}\, \mathcal{P}_{ky} + B_{ky}\, p'_{wy}, & \\
c_k = B_{kx}\, \mathcal{P}_{kx} + B_{ky}\, \mathcal{P}_{ky}, & \\
A_{kx} = (\cos\phi_k - \lambda_k r'_{wx})/\omega_k, & A_{ky} = (\sin\phi_k - \lambda_k r'_{wy})/\omega_k, \\
B_{kx} = x_k - r_{wx} - (z_k - z_c) r'_{wx}, & B_{ky} = y_k - r_{wy} - (z_k - z_c) r'_{wy}, \\
\mathcal{P}_{kx} = [p_{wx} + (z_k - z_c) p'_{wx}]\, \omega_k/\lambda_k, & \mathcal{P}_{ky} = \left[p_{wy} + (z_k - z_c) p'_{wy}\right] \omega_k/\lambda_k.
\end{array} \tag{64}$$

The expected measurement, $h_k(x_k)$, is the drift distance. To evaluate it, we project the position vector in the planar drift system of the wire, $\vec{r}(\Delta t_k) - \vec{w}$, to the measurement axis $\vec{m}$:

$$h_k(x_k) = [\,(\vec{r}(\Delta t_k) - \vec{w}) \cdot \vec{m}\,]\,. \tag{65}$$

To "stretch" the projected value according to the stereo angle, α, we have to replace $\vec{m}$ by $\vec{m}/\cos\alpha$ in the following formulas. The expected measurement is a linear function of the Δt_k:

$$\begin{array}{rcl}
h_k(x_k) & = & \Delta t_k\, \mathcal{C}_k + m_x B_{kx} + m_y B_{ky}, \\
\mathcal{C}_k & = & (m_x A_{kx} + m_y A_{ky})/\omega_k.
\end{array} \tag{66}$$

We approximate the Jacobian, $\partial(h_k)/\partial(x_k)$, by setting its elements which are very close to zero or unity, explicitly to 0 or 1:

$$\begin{array}{l}
\partial(h_k)/\partial(x_k) = \left(\begin{array}{ccccc} \mathbf{1} & \frac{\partial h_k}{\partial z_k} & \frac{\partial h_k}{\partial \phi_k} & \frac{\partial h_k}{\partial \lambda_k} & \mathbf{0} \end{array}\right), \quad \text{for } |\Delta t_k| \geq 10^{-6}, \\
\partial(h_k)/\partial(x_k) = \left(\begin{array}{ccccc} \mathbf{1} & \frac{\partial h_k}{\partial z_k} & \mathbf{0} & \mathbf{0} & \mathbf{0} \end{array}\right), \quad \text{for } |\Delta t_k| < 10^{-6}.
\end{array} \tag{67}$$

Nontrivial elements of the Jacobian are defined in appendix B.

The axial wires of the CTD run parallel to the z–axis and parameters $\vec{r'}_w$ and $\vec{p'}_w$ vanish in (59) and (61), respectively. A condition of the intersection of the trajectory with the "planar drift plane" results in Eq. 62, which has the solution

$$\begin{array}{rcl}
\Delta t_k & = & -b_k/a_k, \\
a_k & = & (\cos\phi_k\, p_{wx} + \sin\phi_k\, p_{wy})/\omega_k, \\
b_k & = & (x_k - r_{wx})\, p_{wx} + (y_k - r_{wy})\, p_{wy}.
\end{array} \tag{68}$$

A measurement vector for an axial wire, m_k, is either one-dimensional (drift distance) or two-dimensional (drift distance and z position). Let's consider the vector of expected measurement, $h_k(x_k)$, for a general, two-dimensional case

$$h_k(x_k) = \begin{pmatrix} h_{k1}(x_k) \\ h_{k2}(x_k) \end{pmatrix}, \tag{69}$$

with the first component (drift distance) and second (z position), which are defined in (65) and (52), respectively:

$$\begin{aligned} h_{k1}(x_k) &= (x_k + \frac{\Delta t_k}{\omega_k}\cos\phi_k - r_{wx})\, m_{wx} + (y_k + \frac{\Delta t_k}{\omega_k}\sin\phi_k - r_{wy})\, m_{wy}, \\ h_{k2}(x_k) &= z_k + \frac{\lambda_k}{\omega_k}\,\Delta t_k. \end{aligned} \tag{70}$$

We approximate the Jacobian, $\partial(h_k)/\partial(x_k)$ as:

$$\partial(h_k)/\partial(x_k) = \begin{pmatrix} \mathbf{1} & \mathbf{0} & \frac{\partial h_{k1}}{\partial \phi_k} & \mathbf{0} & \mathbf{0} \\ \frac{\partial h_{k2}}{\partial u_k} & \mathbf{1} & \frac{\partial h_{k2}}{\partial \phi_k} & \frac{\partial h_{k2}}{\partial \lambda_k} & \mathbf{0} \end{pmatrix}, \quad \text{for} \quad |\Delta t_k| \geq 10^{-6}, \tag{71}$$

and

$$\partial(h_k)/\partial(x_k) = \begin{pmatrix} \mathbf{1} & \mathbf{0} & \mathbf{0} & \mathbf{0} & \mathbf{0} \\ \frac{\partial h_{k2}}{\partial u_k} & \mathbf{1} & \mathbf{0} & \mathbf{0} & \mathbf{0} \end{pmatrix}, \quad \text{for} \quad |\Delta t_k| < 10^{-6}. \tag{72}$$

Elements of the Jacobian are presented in appendix B.

8.4 Cylindrical Parameterization: Process Noise

We evaluate the components of a vector of particle direction, $\vec{n}$, using parameters ϕ, λ:

$$n_x = \frac{\cos\phi}{\sqrt{1+\lambda^2}}, \qquad n_y = \frac{\sin\phi}{\sqrt{1+\lambda^2}}, \qquad n_z = \frac{\lambda}{\sqrt{1+\lambda^2}} \quad \text{and} \quad n_t = \frac{1}{\sqrt{1+\lambda^2}}. \tag{73}$$

We obtain deviations of parameters ϕ, λ, induced by multiple scattering, from Eq. (35):

$$\delta\phi = \theta_1\,\sqrt{1+\lambda^2}, \qquad \delta\lambda = -\theta_2\,\sqrt{1+\lambda^2}, \tag{74}$$

where θ_1, θ_2 are random variables defined by (32). Nonzero elements of the matrix, describing multiple scattering in one scatterer, are:

$$Q_{\phi\phi} = \theta_{ms}^2\,(1+\lambda^2), \qquad Q_{\lambda\lambda} = \theta_{ms}^2\,(1+\lambda^2), \tag{75}$$

with RMS of the deflection angle, θ_{ms}, which is defined by Eq. (33). The matrix, Q_k, in Eq.(18) takes into account a summary effect of multiple scattering:

$$Q_k = \sum_i F_{ik}\, Q_i\, F_{ik}^T, \qquad \text{with} \qquad Fik = \partial(x_k)/\partial(x_i), \tag{76}$$

and, therefore the index i runs over all elements of material on the path from $(k-1)^{th}$ to k^{th} state.

9 Cartesian Parameterization in an Inhomogeneous Magnetic Field

The following choice of track parameters at a reference z–coordinate is suited for forward tracks ($n_z > 0$):

$$\tilde{x}^T = (x,\ y,\ t_x,\ t_y,\ q), \tag{77}$$

where

x = x–coordinate in the Cartesian coordinate system of ZEUS,
y = y–coordinate in the Cartesian coordinate system,
t_x = n_x/n_z track slope in xz–plane,
t_y = n_y/n_z track slope in yz–plane,
q = $Q/|\vec{p}|$, inverse momentum signed according to particle charge, Q.

This parametrization will be called "cartesian". The implementation of the Kalman filter technique in an inhomogeneous magnetic field is analogous to those described in [16]. In the following we discuss the case of forward tracks. The rear tracks are specified in Subsec. 9.7.

9.1 Cartesian Parametrization: Equations of Motion in Inhomogeneous Magnetic Field

For forward tracks we can use the z coordinate as independent variable instead of the path length in Eqs. (29). The equations rewritten w.r.t. z coordinate read:

$$\begin{aligned} dx/dz &= t_x, \\ dy/dz &= t_y, \\ dt_x/dz &= q \cdot \kappa \cdot A_x(t_x, t_y, \vec{B}), \\ dt_y/dz &= q \cdot \kappa \cdot A_y(t_x, t_y, \vec{B}), \\ q &= \text{const}, \end{aligned} \tag{78}$$

where the functions A_x,A_y are

$$\begin{aligned} A_x &= (1 + t_x^2 + t_y^2)^{\frac{1}{2}} \cdot \left[t_y \cdot (t_x B_x + B_z) - (1 + t_x^2) B_y\right], \\ A_y &= (1 + t_x^2 + t_y^2)^{\frac{1}{2}} \cdot \left[-t_x \cdot (t_y B_y + B_z) + (1 + t_y^2) B_x\right]. \end{aligned} \tag{79}$$

To transport track parameters in the inhomogeneous field from plane z_0 to plane z, we solve the latter equations with initial values defined at z_0

$$\tilde{x}_0^T = (x_0,\ y_0,\ t_{x0},\ t_{y0},\ q_0). \tag{80}$$

Three methods are used to solve Eqs. (78), depending on the distance, $s = z - z_o$, between these planes.

1. $|s| < 10$ cm: a parabolic expansion of the particle trajectory is used

$$
\begin{aligned}
x(z) = &\quad x_0 + t_{x0}\cdot s + \tfrac{1}{2}\cdot q_0\cdot\kappa\cdot A_x\cdot s^2,\\
y(z) = &\quad y_0 + t_{y0}\cdot s + \tfrac{1}{2}\cdot q_0\cdot\kappa\cdot A_y\cdot s^2,\\
t_x(z) = &\quad t_{x0} + q_0\cdot\kappa\cdot A_x\cdot s,\\
t_y(z) = &\quad t_{y0} + q_0\cdot\kappa\cdot A_y\cdot s,\\
q(z) = &\quad q_0.
\end{aligned}
\tag{81}
$$

2. 10 cm $\leq |s| <$ 60 cm: the classical fourth-order Runge-Kutta method [14] is selected to find the solution of the equations (78) .

3. $|s| \geq$ 60 cm: a fifth-order Runge-Kutta method with adaptive step size control [14] is used.

9.2 Cartesian Parametrization: Equations for Derivatives

The Jacobian of transformation of parameters given at z_0 to z, $\partial(\tilde{x})/\partial(\tilde{x}_0)$, is defined as:

$$
\partial(\tilde{x})/\partial(\tilde{x}_0) = \begin{pmatrix}
\mathbf{1} & \mathbf{0} & \frac{\partial x}{\partial t_{x0}} & \frac{\partial x}{\partial t_{y0}} & \frac{\partial x}{\partial q_0}\\
\mathbf{0} & \mathbf{1} & \frac{\partial y}{\partial t_{x0}} & \frac{\partial y}{\partial t_{y0}} & \frac{\partial y}{\partial q_0}\\
\mathbf{0} & \mathbf{0} & \mathbf{1} & \frac{\partial t_x}{\partial t_{y0}} & \frac{\partial t_x}{\partial q_0}\\
\mathbf{0} & \mathbf{0} & \frac{\partial t_y}{\partial t_{x0}} & \mathbf{1} & \frac{\partial t_y}{\partial q_0}\\
\mathbf{0} & \mathbf{0} & \mathbf{0} & \mathbf{0} & \mathbf{1},
\end{pmatrix}.
\tag{82}
$$

Elements of the latter Jacobian which are very close to zero or unity, are set to 0 or 1, respectively. Nontrivial elements of the Jacobian (82) for short distance ($|s| <$ 10 cm) we approximate as:

$$
\begin{aligned}
&\partial x/\partial t_{x0} = s, && \partial x/\partial t_{y0} = \tfrac{1}{2}\, q_0\,\kappa\, s^2\,\frac{\partial A_x}{\partial t_{y0}},\\
&\partial y/\partial t_{x0} = \tfrac{1}{2}\, q_0\,\kappa\, s^2\,\frac{\partial A_y}{\partial t_{x0}}, && \partial y/\partial t_{y0} = s,\\
&\partial t_x/\partial t_{y0} = q_0\,\kappa\, s\,\frac{\partial A_x}{\partial t_{y0}}, && \partial t_y/\partial t_{x0} = q_0\,\kappa\, s\,\frac{\partial A_y}{\partial t_{x0}},\\
&\partial x/\partial q_0 = \tfrac{1}{2}\,\kappa\, s^2\, A_x, && \partial y/\partial q_0 = \tfrac{1}{2}\,\kappa\, s^2\, A_y,\\
&\partial t_x/\partial q_0 = \kappa\, s\, A_x, && \partial t_y/\partial q_0 = \kappa\, s\, A_y,
\end{aligned}
\tag{83}
$$

with derivatives $\partial A_x/\partial t_{y0}$ and $\partial A_y/\partial t_{x0}$, which we define below.

To swim derivatives at long distance ($|s| \geq$ 10 cm), we define equations for derivatives as described in [16] and solve them by a Runge-Kutta method simultaneously with equations of motion. The magnetic field is smooth enough even in the STT area and, therefore we regard Eqs. (78) as almost invariant with respect to small shifts by x and y. Derivatives with respect to initial x_0, y_0 are trivial :

$$
\begin{aligned}
\partial\tilde{x}^T/\partial x_0 = &\quad (1,\ 0,\ 0,\ 0,\ 0),\\
\partial\tilde{x}^T/\partial y_0 = &\quad (0,\ 1,\ 0,\ 0,\ 0).
\end{aligned}
$$

To obtain equations for $\partial\tilde{x}/\partial t_{x0}$, we differentiate equations (78) with respect to t_{x0} and change the order of the derivative operators $\partial/\partial t_{x0}$ and d/dz on the left hand sides :

$$\begin{aligned}
d/dz(\partial x/\partial t_{x0}) &= \partial t_x/\partial t_{x0}, \\
d/dz(\partial y/\partial t_{x0}) &= \partial t_y/\partial t_{x0}, \\
d/dz(\partial t_x/\partial t_{x0}) &= q_0 \cdot \kappa \cdot [(\partial A_x/\partial t_x)(\partial t_x/\partial t_{x0}) + (\partial A_x/\partial t_y)(\partial t_y/\partial t_{x0})], \\
d/dz(\partial t_y/\partial t_{x0}) &= q_0 \cdot \kappa \cdot [(\partial A_y/\partial t_x)(\partial t_x/\partial t_{x0}) + (\partial A_y/\partial t_y)(\partial t_y/\partial t_{x0})], \\
\partial q/\partial t_{x0} &= 0,
\end{aligned} \tag{84}$$

where

$$\begin{aligned}
\partial A_x/\partial t_x &= t_x \cdot A_x/(1+t_x^2+t_y^2) + (1+t_x^2+t_y^2)^{\frac{1}{2}} \cdot (t_y \cdot B_x - 2 \cdot t_x \cdot B_y) , \\
\partial A_x/\partial t_y &= t_y \cdot A_x/(1+t_x^2+t_y^2) + (1+t_x^2+t_y^2)^{\frac{1}{2}} \cdot (t_x \cdot B_x + B_z) , \\
\partial A_y/\partial t_x &= t_x \cdot A_y/(1+t_x^2+t_y^2) + (1+t_x^2+t_y^2)^{\frac{1}{2}} \cdot (-t_y \cdot B_y - B_z) , \\
\partial A_y/\partial t_y &= t_y \cdot A_y/(1+t_x^2+t_y^2) + (1+t_x^2+t_y^2)^{\frac{1}{2}} \cdot (-t_x \cdot B_y + 2 \cdot t_y \cdot B_x) .
\end{aligned}$$

Initial values for the solution of latter equations are:

$$\partial\tilde{x}^T/\partial t_{x0} = (0,\ 0,\ 1,\ 0,\ 0). \tag{85}$$

The equations for $\partial\tilde{x}/\partial t_{y0}$ are analogous to Eqs. (84) , but the initial values are :

$$\partial\tilde{x}^T/\partial t_{y0} = \ (0,\ 0,\ 0,\ 1,\ 0) \ .$$

To obtain equations for $\partial\tilde{x}/\partial q_0$, we differentiate Eqs. (78) with respect to q_0 and change the order of the derivative operators $\partial/\partial q_0$ and d/dz in the left parts :

$$\begin{aligned}
d/dz(\partial x/\partial q_0) &= \partial t_x/\partial q_0 \ , \\
d/dz(\partial y/\partial q_0) &= \partial t_y/\partial q_0 \ , \\
d/dz(\partial t_x/\partial q_0) &= \kappa \cdot A_x + \kappa \cdot q_0 \cdot [(\partial A_x/\partial t_x)(\partial t_x/\partial q_0) + (\partial A_x/\partial t_y)(\partial t_y/\partial q_0)] \ , \\
d/dz(\partial t_y/\partial q_0) &= \kappa \cdot A_y + \kappa \cdot q_0 \cdot [(\partial A_y/\partial t_x)(\partial t_x/\partial q_0) + (\partial A_y/\partial t_y)(\partial t_y/\partial q_0)] \ , \\
\partial q/\partial q_0 &= 1 \ .
\end{aligned} \tag{86}$$

Initial values for the solution of latter equations are :

$$\partial\tilde{x}^T/\partial q_0 = (0,\ 0,\ 0,\ 0,\ 1). \tag{87}$$

9.3 Cartesian Parameterization: Projection of State Vector to MVD Measurement

To project a state vector (77) to a BMVD measurement we use the method described in Subsect. 8.2. The state vector, $\tilde{x}_k$, is defined in the reference plane with coordinate, $z = z_k$. We locate the reference plane close to the MVD sensor and, therefore use a linear expansion of the trajectory:

$$\begin{aligned}
x(s_k) &= x_k + t_{xk}\, s_k \\
y(s_k) &= y_k + t_{yk}\, s_k \\
z(s_k) &= z_k + s_k .
\end{aligned} \tag{88}$$

A condition of the trajectory intersection with the sensor plane reads:

$$[\,(\vec{r}(s_k) - \vec{r}_c) \cdot \vec{n}\,] = 0, \tag{89}$$

where $\vec{r}_c$ and $\vec{n}$ are the origin of a local MVD sensor system and the unit vector which is perpendicular to the sensor plane, respectively. The variable advance, Δs_k, to travel from the reference plane at z_k to the sensor plane is:

$$\begin{aligned} \Delta s_k &= -\frac{b_k}{a_k}, \\ a_k &= t_{xk}\, n_x + t_{yk}\, n_y + n_z, \\ b_k &= (x_k - x_c)\, n_x + (y_k - x_c)\, n_y + (z_k - z_c)\, n_z. \end{aligned} \tag{90}$$

Analogous to Eq. 55, we obtain the expected measurement, $h_k(\tilde{x}_k)$, by projecting the position vector in the local frame, $\vec{r}(\Delta s_k) - \vec{r}_c$, to the measurement axis, $\vec{m}$:

$$\begin{aligned} h_k(\tilde{x}_k) &= [\,(\vec{r}(\Delta s_k) - \vec{r}_c) \cdot \vec{m}\,] \\ &= \frac{\Delta s_k}{\omega_k}\, c_k + (x_k - x_c)\, m_x + (y_k - y_c)\, m_y + (z_k - z_c)\, m_z, \\ c_k &= m_x\, t_{xk} + m_y\, t_{yk} + m_z. \end{aligned} \tag{91}$$

Nontrivial elements of the Jacobian, $\partial(h_k)/\partial(\tilde{x}_k)$, are:

$$\begin{aligned} &\partial h_k/\partial x_k = m_x - c_k\, n_x \,/\, a_k, \qquad &&\partial h_k/\partial y_k = m_y - c_k\, n_y \,/\, a_k, \\ &\partial h_k/\partial t_{xk} = \partial h_k/\partial x_k \cdot \Delta s_k, \qquad &&\partial h_k/\partial t_{yk} = \partial h_k/\partial y_k \cdot \Delta s_k. \end{aligned} \tag{92}$$

Derivatives with respect to slopes have an additional order of smallness $o(\Delta s_k)$ and we approximate the Jacobian, $\partial(h_k)/\partial(\tilde{x}_k)$, for the BMVD:

$$\begin{aligned} \partial(h_k)/\partial(\tilde{x}_k) &= \left(\begin{array}{ccccc} \frac{\partial h_k}{\partial x_k} & \frac{\partial h_k}{\partial y_k} & \frac{\partial h_k}{\partial t_{xk}} & \frac{\partial h_k}{\partial t_{yk}} & \mathbf{0} \end{array} \right), \quad \text{for } |\Delta s_k| \geq 10^{-3}, \\ \partial(h_k)/\partial(\tilde{x}_k) &= \left(\begin{array}{ccccc} \frac{\partial h_k}{\partial x_k} & \frac{\partial h_k}{\partial y_k} & \mathbf{0} & \mathbf{0} & \mathbf{0} \end{array} \right), \quad \text{for } |\Delta s_k| < 10^{-3}. \end{aligned} \tag{93}$$

Sensors of the FMVD are almost perpendicular to the z–axis and, therefore $n_{x,y} \approx 0$. We locate the reference plane at the position of the FMVD sensor ($\Delta s_k = 0$). Taking into account latter remarks, we obtain from Eq. (92) the Jacobian, $\partial(h_k)/\partial(\tilde{x}_k)$, for the FMVD

$$\partial(h_k)/\partial(\tilde{x}_k) = \left(\begin{array}{ccccc} m_x & m_y & \mathbf{0} & \mathbf{0} & \mathbf{0} \end{array} \right). \tag{94}$$

9.4 Cartesian Parameterization: Projection of State Vector to CTD Measurement

The linear expansion of a particle trajectory (88) defines the particle coordinates in the immediate vicinity of a stereo wire. An approach to obtain the projection of cartesian

state vector to CTD stereo measurement is similar to those discussed in Subsec. 8.3. A condition of the trajectory intersection with the planar drift plane reads:

$$[\,(\vec{r}(s_k) - \vec{w}) \cdot \vec{n}\,] = 0, \tag{95}$$

where the coordinate of the wire, $\vec{w}$, and vector, $\vec{n}$, are defined by (59) and (61), respectively. The variable advance, Δs_k, to travel from the reference plane to the planar drift plane is a solution of a quadratic equation, $(\Delta s_k)^2\, a_k + \Delta s_k\, b_k + c_k = 0$:

$$\Delta s_k = \frac{1}{2a_k}\left(-b_k + \sqrt{b_k^2 - 4\, a_k\, c_k}\right), \tag{96}$$

with coefficients

$$\begin{array}{ll}
a_k = A_{kx}\, p'_{wx} + A_{ky}\, p'_{wy}, & \\
b_k = A_{kx}\, \mathcal{P}_{kx} + B_{kx}\, p'_{wx} + A_{ky}\, \mathcal{P}_{ky} + B_{ky}\, p'_{wy}, & \\
c_k = B_{kx}\, \mathcal{P}_{kx} + B_{ky}\, \mathcal{P}_{ky}, & \\
A_{kx} = t_{kx} - r'_{wx}, & A_{ky} = t_{ky} - r'_{wy}, \\
B_{kx} = x_k - r_{wx} - (z_k - z_c)\, r'_{wx}, & B_{ky} = y_k - r_{wy} - (z_k - z_c)\, r'_{wy}, \\
\mathcal{P}_{kx} = p_{wx} + (z_k - z_c)\, p'_{wx}, & \mathcal{P}_{ky} = p_{wy} + (z_k - z_c)\, p'_{wy}.
\end{array} \tag{97}$$

We obtain the expected measurement, $h_k(x_k)$, i.e. drift distance, as in (65):

$$\begin{array}{rcl}
h_k(x_k) & = & \left[x_k + t_{kx}\, \Delta s_k - r_{wx} - (z_k - z_c + \Delta s_k)\, r'_{wx}\right]\, m_x \\
& & + \left[y_k + t_{ky}\, \Delta s_k - r_{wy} - (z_k - z_c + \Delta s_k)\, r'_{wy}\right]\, m_y,
\end{array} \tag{98}$$

where the $\vec{m}$ have to by replaced by $\vec{m}/\cos\alpha$ to take into account the stereo angle, α. Derivatives with respect to slopes have an additional order of smallness $o(\Delta s_k)$ and we approximate the Jacobian, $\partial(h_k)/\partial(\tilde{x}_k)$, for the CTD stereo measurement:

$$\begin{array}{l}
\partial(h_k)/\partial(\tilde{x}_k) = \left(\begin{array}{ccccc} \dfrac{\partial h_k}{\partial x_k} & \dfrac{\partial h_k}{\partial y_k} & \dfrac{\partial h_k}{\partial t_{xk}} & \dfrac{\partial h_k}{\partial t_{yk}} & \mathbf{0} \end{array}\right), \quad \text{for } |\Delta s_k| \geq 10^{-3}, \\
\partial(h_k)/\partial(\tilde{x}_k) = \left(\begin{array}{ccccc} \dfrac{\partial h_k}{\partial x_k} & \dfrac{\partial h_k}{\partial y_k} & \mathbf{0} & \mathbf{0} & \mathbf{0} \end{array}\right), \quad \text{for } |\Delta s_k| < 10^{-3}.
\end{array} \tag{99}$$

Elements of the Jacobian, $\partial(h_k)/\partial(\tilde{x}_k)$, are presented in appendix C.

Axial wires of the CTD run parallel to the z–axis and parameters, $\vec{r'}_w$ and $\vec{p'}_w$ vanish in (59) and (61), respectively. A condition of the intersection of the trajectory with the planar drift plane leads to Eq. (95), which has the solution:

$$\begin{array}{rl}
\Delta s_k & = -b_k/a_k, \\
a_k & = t_{xk}\, p_{wx} + t_{yk}\, p_{wy}, \\
b_k & = (x_k - r_{wx})\, p_{wx} + (y_k - r_{wy})\, p_{wy}.
\end{array} \tag{100}$$

We consider the vector of expected measurement, $h_k(x_k)$, for the general, two-dimensional case

$$h_k(x_k) = \left(\begin{array}{c} h_{k1}(x_k) \\ h_{k2}(x_k) \end{array}\right), \tag{101}$$

with the first and second component being a drift distance and z–position, respectively:

$$\begin{array}{l} h_{k1}(x_k) = (x_k + t_{kx}\,\Delta s_k - r_{wx})\; m_x + (y_k + t_{ky}\,\Delta s_k - r_{wy})\; m_y, \\ h_{k2}(x_k) = z_k + \Delta s_k. \end{array} \tag{102}$$

We approximate the Jacobian, $\partial(h_k)/\partial(x_k)$, as:

$$\partial(h_k)/\partial(x_k) = \begin{pmatrix} \frac{\partial h_{k1}}{\partial x_k} & \frac{\partial h_{k1}}{\partial y_k} & \frac{\partial h_{k1}}{\partial t_{kx}} & \frac{\partial h_{k1}}{\partial t_{ky}} & \mathbf{0} \\ \frac{\partial h_{k2}}{\partial x_k} & \frac{\partial h_{k2}}{\partial y_k} & \frac{\partial h_{k2}}{\partial t_{kx}} & \frac{\partial h_{k2}}{\partial t_{ky}} & \mathbf{0} \end{pmatrix}, \quad \text{for} \quad |\Delta s_k| \geq 10^{-3}, \tag{103}$$

and

$$\partial(h_k)/\partial(x_k) = \begin{pmatrix} \frac{\partial h_{k1}}{\partial x_k} & \frac{\partial h_{k2}}{\partial y_k} & \mathbf{0} & \mathbf{0} & \mathbf{0} \\ \frac{\partial h_{k2}}{\partial x_k} & \frac{\partial h_{k2}}{\partial y_k} & \mathbf{0} & \mathbf{0} & \mathbf{0} \end{pmatrix}, \quad \text{for} \quad |\Delta s_k| < 10^{-3}, \tag{104}$$

where we take into account an additional order of smallness $o(\Delta s_k)$ for derivatives with respect to track slopes. We obtain nontrivial elements of latter Jacobians in appendix C.

9.5 Cartesian Parameterization: Projection of State Vector to STT Measurement

Signal wires of a given STT layer are arranged in a plane perpendicular to the z–axis with coordinate $z = z_w$. We locate the reference plane at the position of the layer, i.e. $z_k = z_w$. The particle trajectory inside a straw tube we approximate by a straight line. The latter line and the signal wire are described as lines which pass through points $\vec{r}_k$ and $\vec{r}_w$ and have directions $\vec{n}_k$ and $\vec{n}_w$, respectively:

$$\vec{r}_k = \begin{pmatrix} x_k \\ y_k \\ z_w \end{pmatrix}, \quad \vec{r}_w = \begin{pmatrix} x_w \\ y_w \\ z_w \end{pmatrix}, \quad \vec{n}_k = \begin{pmatrix} n_{kx} \\ n_{ky} \\ n_{kz} \end{pmatrix}, \quad \vec{n}_w = \begin{pmatrix} n_{wx} \\ n_{wy} \\ 0 \end{pmatrix}. \tag{105}$$

Components of the vector of particle direction, $\vec{n}_k$, we calculate using track slopes t_{kx}, t_{ky}:

$$n_{kx} = \frac{t_{kx}}{\sqrt{1 + t_{kx}^2 + t_{ky}^2}}, \quad n_{ky} = \frac{t_{ky}}{\sqrt{1 + t_{kx}^2 + t_{ky}^2}}, \quad n_{kz} = \frac{1}{\sqrt{1 + t_{kx}^2 + t_{ky}^2}}. \tag{106}$$

The expected measurement is a drift distance[2] in the straw, which is evaluated as a distance between these two lines:

$$h_k(\tilde{x}_k) \;\; = \;\; \frac{(\vec{r}_k - \vec{r}_w) \cdot \vec{n}_k \times \vec{n}_w}{|\vec{n}_k \times \vec{n}_w|}. \tag{107}$$

[2] We expect that left–right ambiguity of the drift distance is resolved and, therefore regard it as a signed value.

After simple calculations the expected measurement reads:

$$h_k(\tilde{x}_k) \;=\; \frac{-(x_k - x_w)n_{wy} + (y_k - y_w)n_{wx}}{\sqrt{1 + (t_{kx}\, n_{wy} - t_{ky}\, n_{wx})^2}}. \tag{108}$$

The Jacobian of the latter transformation we can approximate as:

$$\partial(h_k)/\partial(\tilde{x}_k) = \left(\begin{array}{ccccc} \dfrac{\partial h_k}{\partial x_k} & \dfrac{\partial h_k}{\partial y_k} & \mathbf{0} & \mathbf{0} & \mathbf{0} \end{array} \right), \tag{109}$$

with

$$\begin{aligned} \partial h_k/\partial x_k &= -n_{wy} \,/\, \sqrt{1 + (t_{kx}\, n_{wy} - t_{ky}\, n_{wx})^2}, \\ \partial h_k/\partial y_k &= \;\; n_{wx} \,/\, \sqrt{1 + (t_{kx}\, n_{wy} - t_{ky}\, n_{wx})^2}. \end{aligned} \tag{110}$$

9.6 Cartesian Parameterization: Process Noise

We evaluate deviations of track slopes induced by multiple scattering from Eq. (35):

$$\begin{aligned} \delta t_{kx} = \delta\left(\frac{n_{kx}}{n_{kz}}\right) &= -\theta_1 \frac{n_{ky}}{n_{kz}\, n_{kt}} + \theta_2 \frac{n_{kx}}{n_{kz}^2\, n_{kt}}, \\ \delta t_{ky} = \delta\left(\frac{n_{ky}}{n_{kz}}\right) &= \;\; \theta_1 \frac{n_{kx}}{n_{kz}\, n_{kt}} + \theta_2 \frac{n_{ky}}{n_{kz}^2\, n_{kt}}, \end{aligned} \tag{111}$$

where θ_1, θ_2 are random variables defined by (32). Nonzero elements of the matrix describing multiple scattering in one scatterer are:

$$\begin{aligned} Q_{t_x\, t_x} &= \theta_{ms}^2\, (1 + t_{kx}^2)\, (1 + t_{kx}^2 + t_{ky}^2), \\ Q_{t_y\, t_y} &= \theta_{ms}^2\, (1 + t_{ky}^2)\, (1 + t_{kx}^2 + t_{ky}^2), \\ Q_{t_x\, t_y} &= \theta_{ms}^2\, t_{kx}\, t_{ky}\, (1 + t_{kx}^2 + t_{ky}^2), \end{aligned} \tag{112}$$

with RMS of the deflection angle, θ_{ms}, which is defined by Eq. (33). The matrix, Q_k, in prediction equation (18) has to account for a summary effect of multiple scattering on a path from $(k-1)^{th}$ to k^{th} state, and is therefore evaluated analogous to (76).

9.7 Cartesian Parameterization for Rear Tracks

For rear tracks ($n_z < 0$) we use a parameterization analogous to those for forward tracks. The meaning of parameters x, y, q is identical with (77). For rear tracks we define slopes w.r.t. negative direction of the z–axis:

$$\begin{aligned} t_x &= -n_x \,/\, n_z, \\ t_y &= -n_y \,/\, n_z. \end{aligned} \tag{113}$$

Equations of particle motion for rear tracks are identical to (78) for forward tracks, but with slightly different definition of functions A_x,A_y:

$$\begin{aligned} A_x &= (1 + t_x^2 + t_y^2)^{\frac{1}{2}} \cdot \left[t_y \cdot (-t_x B_x + B_z) + (1 + t_x^2) B_y \right], \\ A_y &= (1 + t_x^2 + t_y^2)^{\frac{1}{2}} \cdot \left[-t_x \cdot (-t_y B_y + B_z) - (1 + t_y^2) B_x \right]. \end{aligned} \tag{114}$$

Equations (88) for linear and (81) for parabolic expansions of trajectory can be used for rear tracks also, if we regard the expansion w.r.t. z–coordinate decrement, $s = z_0 - z$.

10 Global Parameterization

A global perigee parameterization of tracks [13] is used for analyses in the ZEUS experiment. The perigee parameters are parameters of a helix, which are defined at the track's point of closest approach to the z–axis:

$$\tilde{x}^T = (\phi_H,\ Q/R_H,\ QD_H,\ z_H,\ \cot\theta)\,, \tag{115}$$

where

ϕ_H = angle of xy–projection of track direction with the x–axis,
Q/R_H = helix curvature signed by a particle charge, Q,
QD_H = signed minimal distance to z–axis,
z_H = z–coordinate at point of closest approach,
$\cot\theta$ = cotangent of track direction w.r.t. z-axis.

Transformations between local parameters (cylindrical or cartesian) and global ZEUS perigee parameters are given in appendix D.

11 Fast Computations with Kalman Filter Technique

Most of the calculation by the Kalman filter technique is in the following procedures:

- transportation and projection of track parameters (24) and evaluation of Jacobian matrices (25);
- matrix operations in prediction (18), filter (21) and smoother (23) equations;
- search of a track crossing with material to evaluate effects of multiple scattering and energy loss.

Approaches to fast computation with Kalman filter technique were discussed for the magnet tracking [17],[18] at the HERA-B detector.

To reduce computations we use a flexible strategy for propagating track parameters and derivatives in the inhomogeneous field, as described for forward and rear tracks in Subsec. 9.1. For long ($s > 10\,\mathrm{cm}$) distances we use numerical integration of the equations of motion, but integrate derivatives together with a "zero trajectory" that allows to reduce computations. For short distances ($s < 10\,\mathrm{cm}$) we use parabolic expansion (81) of the particle trajectory, which is very fast in computations.

To keep the computational effort at a minimum we exploit the sparse structures of the Jacobian matrices. The Jacobian of track propagation includes elements which are very close to 0 or 1, therefore we use Jacobian approximations and set such elements to 0 or 1. The Jacobians for cylindrical (51) and cartesian (82) parameterization contain only 11 and 10 nontrivial elements, respectively. To calculate the product of matrices $F_k\, C_{k-1}\, F_k^T$ in (18) we implement functions, which take into account a sparse structure

of the matrix F_k. For example, the function for 10 nontrivial elements of the F_k implies 73 multiplications, which is much smaller than 200 multiplications needed for the case of the completely filled matrix F_k of size 5 by 5.

The Jacobians of projection transformation, H_k, are approximated also, as shown in (58), (67), (71), (72) etc. We implement corresponding functions for the calculation of products of $C_k^{k-1} H_k^T$ and $(1 - K_k H_k) C_k^{k-1}$ in (21) or $(1 - H_k K_k) V_k$ in (22). These functions take into account the sparse structure of the matrix H_k. For example, only 20 multiplications are sufficient to obtain the matrix $(1-K_k H_k) C_k^{k-1}$ for the option with one nontrivial element in the matrix H_k. This has to be compared with 100 multiplications needed for the completely filled matrix of size 5 by 1.

To evaluate the effects of multiple scattering and energy loss, we describe the distribution of material in the ZEUS inner trackers by using about 1800 separate volumes. After crossing a given volume, a particle can reach only a limited number of other volumes. We implement an approach called *volume navigation* [19] for fast search of a track's crossings with these volumes. Using the Monte Carlo technique, we evaluate for each volume a list of volumes, which can be crossed subsequently. On average, one list includes about 7 subsequent volumes. The lists are used to navigate a fast search of track crossing with volumes.

The described approaches have been programmed [20] in C++. We follow recipes of effective programming of numerical calculations [14] and implement STL containers to store objects like hits, states, tracks etc.

Table 1: Computing time of the track fit per ZEUS event on a PC with processor Intel CPU 3.06GHz for different groups of tracks.

Fitted tracks	Fraction	Field model	Time/event
Forward ($\theta < 60°$)	59%	inhomogeneous	12 ms
Central ($60° < \theta < 120°$)	23%	homogeneous	7 ms
Rear ($\theta > 120°$)	18%	inhomogeneous	1 ms
All tracks in event	100%	(in)homogeneous	20 ms

A ZEUS event contains up to 100 fitted tracks and about 30 tracks on average. The longest tracks include about 80 hits in the central area, 50 hits in a transition region and 30 hits in the very forward direction. Fitting all the tracks in one event takes 20 ms on PC with processor Intel CPU 3.06GHz (see Table 1) and 46 ms with processor Intel CPU 1GHz. About of 77% of tracks are fitted using the inhomogeneous field as shown in Table 1. The computing time for these tracks is comparable with those which are fitted using the homogeneous field approximation.

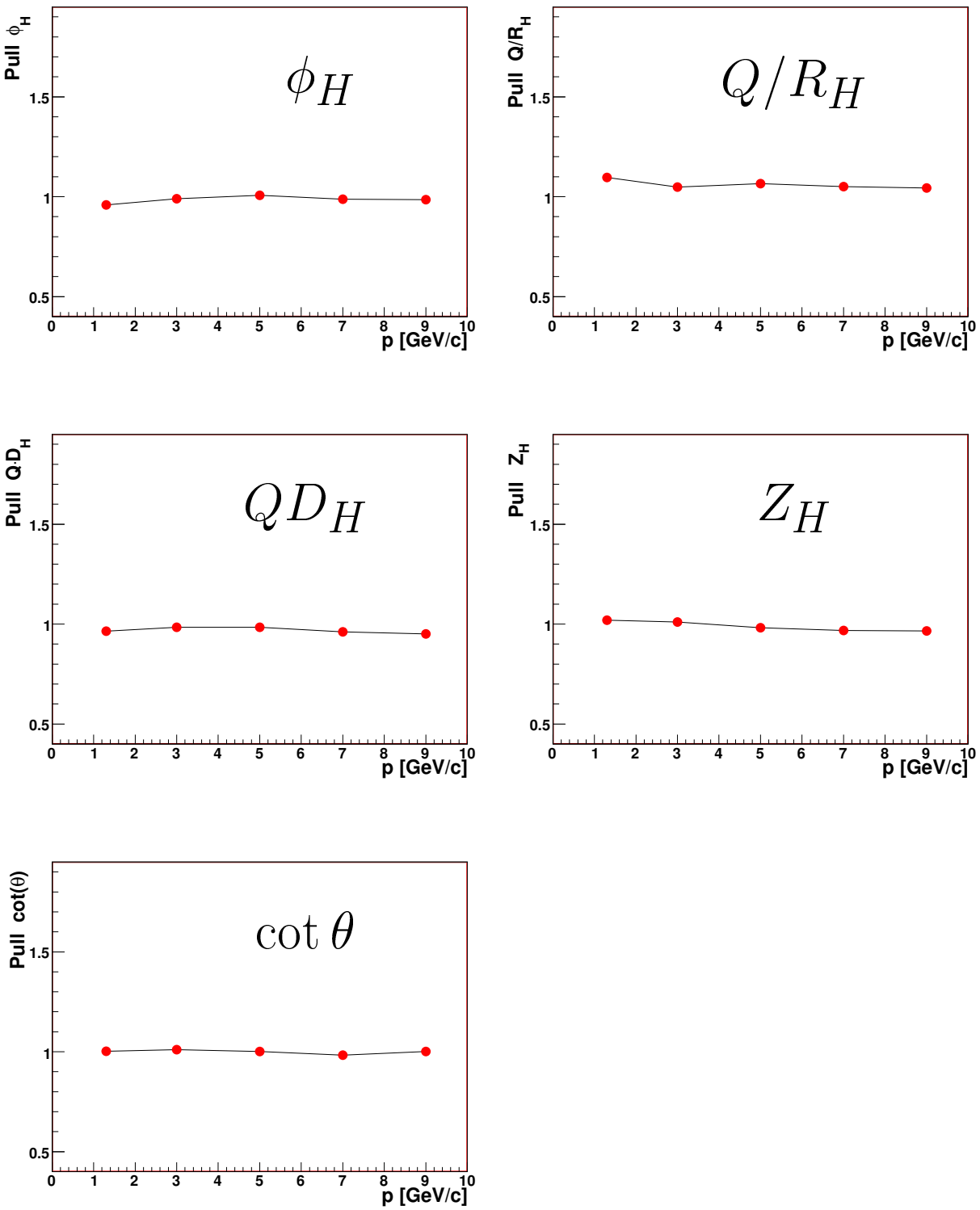

Figure 1: Standard deviations of the pull distributions of fitted track parameters in perigee parameterization (115) for MC simulated muons versus the momentum.

The precision of fitted parameters depends on the resolution and details of the performance of the ZEUS trackers and will be discussed in the next note [20]. Here we would like to mention that approximations implemented to reduce computations, are not made at the expense of track parameter precision. Evaluation of the covariance matrices of fitted parameters in (21) and (23) are the most complicated computations, including operation with the transport, projection and process noise matrices. Calculated variances of these matrices are in good agreement with the residuals of the fitted parameters. Standard deviations of pull distribution (residuals normalized by their estimated error) are close to unity for different track momenta, as shown in Fig. 1.

12 Conclusions

We consider a mathematical framework for the rigorous approach to a common track fit using the trackers in the inner region of the ZEUS detector: CTD, BMVD, FMVD and STT. We discuss track models and likelihood functions in such a multi-component tracker. The approach offers a rigorous treatment of field inhomogeneity, multiple scattering and energy loss. The track fitting procedure makes use of the Kalman filter technique.

We describe details of the mathematics for the fast implementation of a Kalman filter for the cylindrical drift chamber, barrel and forward silicon strip detectors and straw drift chambers. The cases of homogeneous and inhomogeneous field are considered.

We discuss how to reduce computations and make the track fitting procedure fast. Average computing time of track fitting in one ZEUS event is about of 20 ms on a PC with processor Intel CPU 3.06GHz.

Acknowledgments: Fruitful discussions with R. Mankel helped me a lot to finalize the results. Cordial thanks to A. Antonov, C. Catteral and G. Hartner for their expertise on the implementation of ZEUS trackers in the simulation and reconstruction software. I am grateful to O. Behnke and G. Hartner for the careful reading of the manuscript. I would like to thank the ZEUS group at DESY for the kind hospitality extended to me during my visit.

References

[1] ZEUS Coll., U. Holm (ed.), *The ZEUS Detector.* Status Report (unpublished), DESY (1993), `http://www-zeus.desy.de/bluebook/bluebook.html`

[2] A. Polini et al., Nucl. Instr. and Meth. **A581** (2007) 656

[3] B. Foster et al., Nucl. Instr. and Meth. **A228** (1994) 254

[4] S. Fourletov (ZEUS STT Collaboration), Nucl. Instr. and Meth. **A535** (2004) 191

[5] By ZEUS Collaboration (R. Mankel for the collaboration), *Alignment of the ZEUS micro-vertex detector,* Prepared for 1st LHC Detection Alignment Workshop, Geneva, 4-6 Sep 2006. Published in "Geneva 2006, LHC detector alignment" (2006) 51

[6] V.P. Zhigunov, S.G. Nikitin, V.F. Perelygin and A.A. Spiridonov, Nucl. Instr. and Meth. **179** (1981) 427

[7] V. Blobel, Nucl. Instr. and Meth. **A566** (2006) 14

[8] P. Billoir, Nucl. Instr. and Meth. **225** (1984) 352

[9] R. Frühwirth, Nucl. Instr. and Meth. **A262** (1987) 444

[10] R.E. Kalman, Trans. ASME, J. Basic Engineering (1960)
R. Battin, Am. Rocket Soc. 32 (1962) 1681
R.E. Kalman and R.S. Bucy, Trans. ASME, J. Basic Engineering (1962)

[11] R. Mankel, Rep. Prog. Phys. **67** (2004) 553

[12] T. Lohse, W. Witzeling, Adv. Ser. Direct. High Energy Phys. **9** (1992) 81

[13] G. Hartner, *VCTRAK Briefing: Program and Math,* ZEUS note 98-058 (1998)

[14] W. Press, S. Teukolsky, W. Vetterling and B. Flannery, *Numerical Recipes in C,* Cambridge University Press, Cambridge (1992)

[15] K. Hagiward et al., Phys. Rev., **D66** (2002) 010001.;

[16] A. Spiridonov, *Optimized Integration of the Equations of Motion of a Particle in the HERA-B Magnet*, HERA-B note 98-113 (1998), physics/0511177

[17] R. Mankel and A. Spiridonov, Nucl. Instr. and Meth. **A426** (1999) 268

[18] A. Spiridonov, Nucl. Instr. and Meth. **A566** (2006) 153

[19] R. Mankel, Nucl. Instr. and Meth. **A395** (1997) 169

[20] A. Spiridonov, *Implementation and Performance of Rigorous Track Fit for the ZEUS Detector*, ZEUS note in preparation

13 Appendix A: Jacobian of prediction transformation in cylindrical parameterization

We use derivatives of t_k to calculate the Jacobian (51) of prediction transformation (49):

$$\begin{aligned}
\partial t_k/\partial u_k &= \frac{\cos(\phi_k - \frac{u_k}{r_k}) - \cos(\phi_k - \frac{u_k}{r_k} - t_k)}{r_k\,\cos(\phi_k - \frac{u_k}{r_k} - t_k) + \frac{1}{\omega_k}\sin t_k},\\
\partial t_k/\partial z_k &= 0,\\
\partial t_k/\partial \phi_k &= -r_k\;\partial t_k/\partial u_k,\\
\partial t_k/\partial \lambda_k &= \frac{\omega_k\lambda_k}{1+\lambda_k^2}\,\partial t_k/\partial \omega_k,\\
\partial t_k/\partial \omega_k &= \frac{2\,(1-\cos t_k) + r_k\,\omega_k\left[\sin(\phi - \frac{u_k}{r_k}) - \sin(\phi - \frac{u_k}{r_k} - t_k)\right]}{r_k\,\omega_k^2\,\cos(\phi - \frac{u_k}{r_k} - t_k) + \omega_k\,\sin t_k}.
\end{aligned} \tag{116}$$

Nontrivial elements of the Jacobian are:

$$\begin{aligned}
\partial u_{k+1}/\partial u_k &= \tfrac{r_{k+1}}{x_{k+1}}\left[\cos\tfrac{u_k}{r_k} + \tfrac{1}{\omega_k}\sin(\phi_k - t_k)\,\partial t_k/\partial u_k\right]\\
&= \tfrac{r_{k+1}}{y_{k+1}}\left[\sin\tfrac{u_k}{r_k} - \tfrac{1}{\omega_k}\cos(\phi_k - t_k)\,\partial t_k/\partial u_k\right],\\
\partial u_{k+1}/\partial \phi_k &= \tfrac{r_{k+1}}{\omega_k\,x_{k+1}}\left[\sin\phi_k - \sin(\phi_k - t_k)\,(1 - \partial t_k/\partial\phi_k)\right]\\
&= \tfrac{r_{k+1}}{\omega_k\,y_{k+1}}\left[-\cos\phi_k + \cos(\phi_k - t_k)\,(1 - \partial t_k/\partial\phi_k)\right],\\
\partial u_{k+1}/\partial \lambda_k &= \tfrac{r_{k+1}}{\omega_k\,x_{k+1}}\left[-\tfrac{\lambda_k}{1+\lambda_k^2}\left(\cos(\phi_k - t_k) - \cos\phi_k\right) + \sin(\phi_k - t_k)\,\partial t_k/\partial\lambda_k\right]\\
&= \tfrac{r_{k+1}}{\omega_k\,y_{k+1}}\left[-\tfrac{\lambda_k}{1+\lambda_k^2}\left(\sin(\phi_k - t_k) - \sin\phi_k\right) - \cos(\phi_k - t_k)\,\partial t_k/\partial\lambda_k\right],\\
\partial u_{k+1}/\partial q_k &= \tfrac{r_{k+1}}{q_k\,\omega_k\,x_{k+1}}\left[\cos\phi_k - \cos(\phi_k - t_k) + \omega_k\,\sin(\phi_k - t_k)\,\partial t_k/\partial\omega_k\right]\\
&= \tfrac{r_{k+1}}{q_k\,\omega_k\,y_{k+1}}\left[\sin\phi_k - \sin(\phi_k - t_k) - \omega_k\,\cos(\phi_k - t_k)\,\partial t_k/\partial\omega_k\right],
\end{aligned}$$

$$\begin{aligned}
\partial z_{k+1}/\partial u_k &= \tfrac{\lambda_k}{\omega_k}\,\partial t_k/\partial u_k, & \partial z_{k+1}/\partial \phi_k &= \tfrac{\lambda_k}{\omega_k}\,\partial t_k/\partial \phi_k,\\
\partial z_{k+1}/\partial \lambda_k &= \tfrac{t_k}{\omega_k}, & \partial z_{k+1}/\partial q_k &= \tfrac{\lambda_k}{q_k}\left(\partial t_k/\partial\omega_k - \tfrac{t_k}{\omega_k}\right),\\
\partial \phi_{k+1}/\partial u_k &= -\partial t_k/\partial u_k, & \partial \phi_{k+1}/\partial \lambda_k &= \frac{\lambda_k\omega_k}{1+\lambda_k^2}\partial t_k/\partial\omega_k,\\
\partial \phi_{k+1}/\partial q_k &= -\partial t_k/\partial q_k.
\end{aligned} \tag{117}$$

14 Appendix B: Jacobian of projection transformation for the CTD in cylindrical parameterization

Elements of the Jacobian (67) of projection transformation (66) for the stereo CTD are:

$$\begin{aligned}
\partial h_k/\partial z_k &= \mathcal{C}_k\,\partial\Delta t_k/\partial z_k - m_x\,r'_{wx} - m_y\,r'_{wy},\\
\partial h_k/\partial \phi_k &= \mathcal{C}_k\,\partial\Delta t_k/\partial \phi_k + \frac{\Delta t_k}{\omega_k}\left(-m_x\,\sin\phi_k + m_y\,\cos\phi_k\right),\\
\partial h_k/\partial \lambda_k &= \mathcal{C}_k\,\partial\Delta t_k/\partial \lambda_k - \Delta t_k\left[\frac{\lambda_k\,\mathcal{C}_k}{1+\lambda_k^2} + \frac{1}{\omega_k}\left(m_x\,r'_{wx} + m_y\,r'_{wy}\right)\right],
\end{aligned} \tag{118}$$

with derivatives

$$\begin{aligned}
\partial\Delta t_k/\partial z_k &= -\frac{\Delta t_k\,\partial b_k/\partial z_k + \partial c_k/\partial z_k}{2\,\Delta t_k\,a_k + b_k},\\
\partial\Delta t_k/\partial \phi_k &= -\frac{\Delta t_k\,\partial b_k/\partial \phi_k}{{\Delta t_k}^2\,\partial a_k/\partial \phi_k + 2\,\Delta t_k\,a_k + b_k},\\
\partial\Delta t_k/\partial \lambda_k &= -\frac{\Delta t_k\,\partial b_k/\partial \lambda_k + \partial c_k/\partial \lambda_k}{{\Delta t_k}^2\,\partial a_k/\partial \lambda_k + 2\,\Delta t_k\,a_k + b_k},\\
\partial b_k/\partial z_k &= \frac{\omega_k}{\lambda_k}\left(A_{kx}\,p'_{wx} + A_{ky}\,p'_{wy}\right) - p'_{wx}\,r'_{wx} - p'_{wy}\,r'_{wy},\\
\partial c_k/\partial z_k &= \frac{\omega_k}{\lambda_k}\left(B_{kx}\,p'_{wx} + B_{ky}\,p'_{wy}\right) - \mathcal{P}_{kx}\,r'_{wx} - \mathcal{P}_{ky}\,r'_{wy},\\
\partial a_k/\partial \phi_k &= \frac{1}{\omega_k}\left(-\sin\phi_k\,p'_{wx} + \cos\phi_k\,p'_{wy}\right),\\
\partial b_k/\partial \phi_k &= \frac{1}{\omega_k}\left(-\sin\phi_k\,\mathcal{P}_{kx} + \cos\phi_k\,\mathcal{P}_{ky}\right),\\
\partial a_k/\partial \lambda_k &= p'_{wx}\,\partial A_{kx}/\partial\lambda_k + p'_{wy}\,\partial A_{ky}/\partial\lambda_k,\\
\partial b_k/\partial \lambda_k &= \mathcal{P}_{kx}\,\partial A_{kx}/\partial\lambda_k + \mathcal{P}_{ky}\,\partial A_{ky}/\partial\lambda_k\\
&\quad - \frac{1}{\lambda_k\,(1+\lambda_k^2)}\left(A_{kx}\,\mathcal{P}_{kx} + A_{ky}\,\mathcal{P}_{ky}\right),\\
\partial c_k/\partial \lambda_k &= -\frac{1}{\lambda_k\,(1+\lambda_k^2)}\left(B_{kx}\,\mathcal{P}_{kx} + B_{ky}\,\mathcal{P}_{ky}\right),\\
\partial A_{kx}/\partial \lambda_k &= -\frac{1}{\omega_k}\left[\frac{\lambda_k}{1+\lambda_k^2}(\cos\phi_k - \lambda_k r'_{wx}) + r'_{wx}\right],\\
\partial A_{ky}/\partial \lambda_k &= -\frac{1}{\omega_k}\left[\frac{\lambda_k}{1+\lambda_k^2}(\sin\phi_k - \lambda_k r'_{wy}) + r'_{wy}\right].
\end{aligned} \tag{119}$$

Elements of the corresponding Jacobian (71) for the axial CTD look as:

$$\begin{aligned}
\partial h_{k1}/\partial \phi_k &= \frac{m_{wx}}{\omega_k}\left(-\Delta t_k\sin\phi_k + \frac{\partial\Delta t_k}{\partial\phi_k}\,\cos\phi_k\right)\\
&\qquad + \frac{m_{wy}}{\omega_k}\left(\Delta t_k\cos\phi_k + \frac{\partial\Delta t_k}{\partial\phi_k}\,\sin\phi_k\right),\\
\partial h_{k2}/\partial u_k &= \frac{\lambda_k}{a_k\,\omega_k}(p_{wx}\frac{y_k}{r_k} - p_{wy}\frac{x_k}{r_k}),\\
\partial h_{k2}/\partial \phi_k &= \frac{\lambda_k}{\omega_k}\,\frac{\partial\Delta t_k}{\partial\phi_k},\\
\partial h_{k2}/\partial \lambda_k &= \frac{\Delta t_k}{\omega_k},\\
\partial\Delta t_k/\partial \phi_k &= \frac{\Delta t_k}{a_k\,\omega_k}(p_{wx}\,\sin\phi_k - p_{wy}\,\cos\phi_k).
\end{aligned} \tag{120}$$

15 Appendix C: Jacobian of projection transformation for the CTD in cartesian parameterization

Nontrivial elements of the Jacobian (99) of projection transformation (98) for the stereo CTD are:

$$\begin{aligned} \partial h_k/\partial x_k &= m_x + M_w \frac{\partial \Delta s_k}{\partial x_k}, & \partial h_k/\partial y_k &= m_y + M_w \frac{\partial \Delta s_k}{\partial y_k}, \\ \partial h_k/\partial t_{xk} &= \frac{\partial h_k}{\partial x_k} \cdot \Delta s_k, & \partial h_k/\partial t_{yk} &= \frac{\partial h_k}{\partial y_k} \cdot \Delta s_k, \end{aligned} \tag{121}$$

with

$$\begin{aligned} \partial \Delta s_k/\partial x_k &= -\frac{\Delta s_k\, p'_{wx} + \mathcal{P}_{kx}}{2\,\Delta s_k\, a_k + b_k}, & \partial \Delta s_k/\partial y_k &= -\frac{\Delta s_k\, p'_{wy} + \mathcal{P}_{ky}}{2\,\Delta s_k\, a_k + b_k}, \\ M_w &= m_{wx}\,(t_{kx} - r'_{wx}) + m_{wy}\,(t_{ky} - r'_{wy}). \end{aligned}$$

Elements of the corresponding Jacobian (103) for the axial CTD read as:

$$\begin{aligned} \partial h_{k1}/\partial x_k &= m_x + M_w \frac{\partial \Delta s_k}{\partial x_k}, & \frac{\partial h_{k1}}{\partial y_k} &= m_y + M_w \frac{\partial \Delta s_k}{\partial y_k}, \\ \partial h_{k1}/\partial t_{xk} &= \frac{\partial h_{k1}}{\partial x_k} \cdot \Delta s_k, & \frac{\partial h_{k1}}{\partial t_{yk}} &= \frac{\partial h_{k1}}{\partial y_k} \cdot \Delta s_k, \\ \partial h_{k2}/\partial x_k &= \frac{\partial \Delta s_k}{\partial x_k}, & \frac{\partial h_{k2}}{\partial y_k} &= \frac{\partial \Delta s_k}{\partial y_k}, \\ \partial h_{k2}/\partial t_{xk} &= \frac{\partial \Delta s_k}{\partial x_k} \cdot \Delta s_k, & \frac{\partial h_{k2}}{\partial t_{yk}} &= \frac{\partial \Delta s_k}{\partial y_k} \cdot \Delta s_k, \end{aligned} \tag{122}$$

with

$$\begin{aligned} \partial \Delta s_k/\partial x_k &= -\frac{p_{wx}}{a_k}, & \partial \Delta s_k/\partial y_k &= -\frac{p_{wy}}{a_k}, \\ M_w &= m_{wx}\, t_{kx} + m_{wy}\, t_{ky}. \end{aligned}$$

16 Appendix D: Conversions from Local to Global Parameters

Track parameters, $u_0, z_0, \phi_0, \lambda_0, q_0$, at the beginning of a central track, which is fitted using the cylindrical parameterization (48), are converted to perigee parameters (115):

$$\begin{aligned} \phi_H &= \phi_0 - t_H\,, \\ Q/R_H &= \kappa\, B_z\, q_0\, \sqrt{1+\lambda_0^2}, \\ QD_H &= -r_0 \sin(\frac{u_0}{r_0} - \phi_0 + t_H) + (\cos t_H - 1)\,/\,(Q/R_H), \\ z_H &= z_0 + \lambda_0\, t_H\,/\,(Q/R_H), \\ \cot\theta &= \lambda_0, \end{aligned} \tag{123}$$

where

$$t_H = \arctan\left[\frac{1/(Q/R_H) - r_0\, \sin(u_0/r_0 - \phi_0)}{r_0\, \cos(u_0/r_0 - \phi_0)}\right] - \frac{\pi}{2}\,\mathrm{sign}(Q/R_H).$$

We convert fitted cartesian parameters at the beginning of a forward track ,$x_0, y_0, t_{0x}, t_{0y}, q_0$, into perigee parameters (115):

$$\begin{aligned}
\phi_H &= \arctan\frac{\mathcal{Y}_0}{\mathcal{X}_0},\\
Q/R_H &= \kappa\, B_z\, q_0\, \frac{\sqrt{1+t_{0x}^2+t_{0y}^2}}{\sqrt{t_{0x}^2+t_{0y}^2}},\\
QD_H &= \frac{-1+\mathcal{Y}_0\,\sin\phi_H+\mathcal{X}_0\,\cos\phi_H}{Q/R_H},\\
z_H &= z_0+\frac{\Phi_0-\phi_H}{\sqrt{t_{0x}^2+t_{0y}^2}\;Q/R_H},\\
\cot\theta_H &= \frac{1}{\sqrt{t_{0x}^2+t_{0y}^2}},
\end{aligned} \tag{124}$$

where

$$\begin{aligned}
\Phi_0 &= \arctan\frac{t_{0y}}{t_{0x}},\\
\mathcal{X}_0 &= -y_0\,Q/R_H+\frac{t_{0x}}{\sqrt{t_{0x}^2+t_{0y}^2}},\\
\mathcal{Y}_0 &= x_0\,Q/R_H+\frac{t_{0y}}{\sqrt{t_{0x}^2+t_{0y}^2}}.
\end{aligned}$$

The transformation from cartesian to perigee parameterization for rear tracks is similar to (124) for parameters $\phi_H, Q/R_H, QD_H$, but differs for parameters z_H and $\cot\theta_H$:

$$\begin{aligned}
z_H &= z_0-\frac{\Phi_0-\phi_H}{\sqrt{t_{0x}^2+t_{0y}^2}\;Q/R_H},\\
\cot\theta_H &= -\frac{1}{\sqrt{t_{0x}^2+t_{0y}^2}}.
\end{aligned} \tag{125}$$